Electronic Supporting Information

Synthesis of Tröger Base-Based[3]arenes for Efficient Iodine Adsorption

Pengbo Niu, [a] Conghao Shi, [a] Jianmin Jiao, [a] Wang Xie, [a] Heng Qiu, [a] Zhen Yang, [a] Juli Jiang, [*a,b] and Leyong Wang [*a]

[a] State Key Laboratory of Analytical Chemistry for Life Science, Jiangsu Key Laboratory of Advanced Organic Materials, School of Chemistry and Chemical Engineering, Nanjing University, Nanjing, 210023, China

[b] Ma' anshan High-Tech Research Institute of Nanjing University, Ma' anshan, 238200, China

* Corresponding Author: jjl@nju.edu.cn; lywang@nju.edu.cn

Table of Contents

1. General Information

All reactions were performed in air atmosphere unless otherwise stated. All chemicals and solvents were purchased from commercial suppliers and were used without further purification unless otherwise specified. Hydroxyl TB were synthesized according to the previously reported literature. All yields were given as isolated yields. NMR spectra were recorded on Bruker DPX 400 MHz or Bruker DPX 500 MHz spectrometer with internal standard tetramethylsilane (TMS) and solvent signals as internal references at 298 K, and the chemical shifts (δ) were expressed in ppm and J values were given in Hz. High-resolution electrospray ionization mass spectra (HR-ESI-MS) were recorded on Bruker micrOTOF-Q III and Agilent 6540Q-TOF LCMS equipped with an electrospray ionization (ESI) probe operating in positive-ion mode with direct infusion. EA were measured on Elementar Vario MICRO cube. The measurements of $[\alpha]_D$ were recorded on AUTOPOL III. The UV-Vis absorption spectra were measured on a Shimadzu UV-3600 UV-Vis Spectrometer. The Fourier Transform Infrared (FT-IR) spectra were recorded in the range 4000-400 cm^{-1} on a Tensor 27 FT-IR spectrophotometer. The Scanning Electron Mircoscopy (SEM) experiments was carried out on a JEOL JSM-6490 instrument. X-ray photoelectron spectroscopy (XPS) experiments were carried out on PHI5000 VersaProbe analyzer. The sample was degassed under vacuum at 100 °C for 5 hours before measurement. Thermogravimetric Analysis (TGA) was carried out using a ASAP2020 analyzer. The samples were heated at the rate of 10 °C/min and N_2 was used as protective gas. The crystal structures were determined by single-crystal X-ray analysis. Data collections were performed using a Bruker Apex Smart CCD diffractometer. The structures were solved with direct methods using the SHELXTL program and refined anisotropically with SHELXTL using full-matrix least-squares procedures.

2. Synthesis and Characterization of M[3], E[3] and B[3]

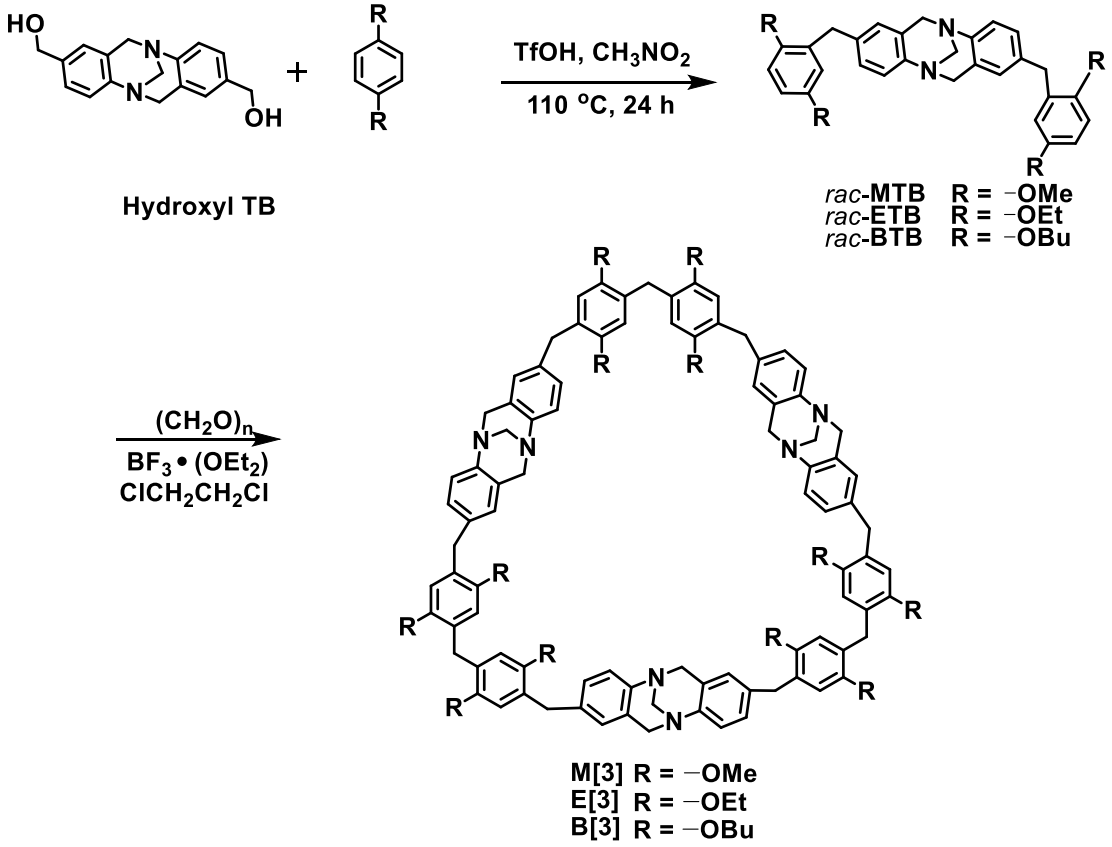

Scheme S1 Synthetic route of **M[3]**, **E[3]** and **B[3]**

Synthesis of *rac*- MTB and characterization data

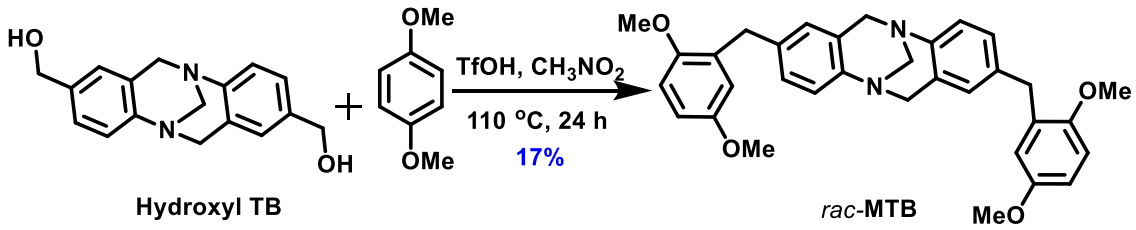

Hydroxyl TB was synthesized according to previous work.[1] To the solution of **Hydroxyl TB** (0.28 g, 1.0 mmol) and 1,4-Dimethoxybenzene (0.80 g, 5.8 mmol) in CH_3NO_2 (50 mL) was added trifluoromethanesulfonic acid (0.2 mL). The mixture was stirred at 110 °C for 24 h. Then the solvent was concentrated by rotary evaporation. The residue was purified by column chromatography on silica gel (eluent: 3/1, v/v, dichloromethane : ethyl acetate) to afford *rac*-**MTB** (0.090 g, 17%), as a yellow solid. ^{1}H NMR (400 MHz, $CDCl_3$) δ 7.02 (s, 4H), 6.78 (d, *J* = 8.8 Hz, 2H), 6.72 (s, 2H), 6.70 (dd, *J* = 8.8, 3.0 Hz, 2H), 6.62 (d, *J* = 3.0 Hz, 2H), 4.64 (d, *J* = 16.7 Hz, 2H), 4.28 (s, 2H), 4.09 (d, *J* = 16.7 Hz, 2H), 3.81 (s, 4H), 3.74 (s, 6H), 3.70 (s, 6H). ^{13}C NMR (100 MHz, $CDCl_3$) δ 153.5, 151.6, 145.5, 136.7, 130.7, 128.0, 127.4, 127.0, 124.9, 116.9, 111.4, 111.2, 66.9, 58.5, 56.0, 55.6, 35.4.

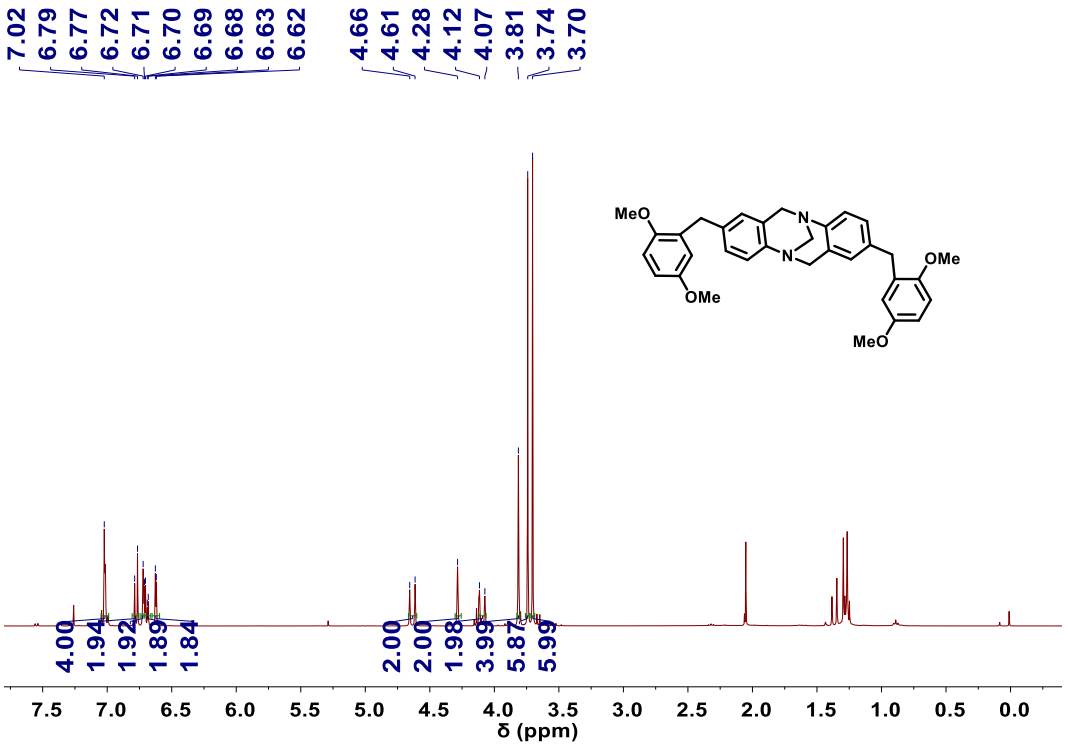

Fig. S1 ^{1}H NMR spectrum (400 MHz, $CDCl_3$, 298 K) of *rac*-**MTB**.

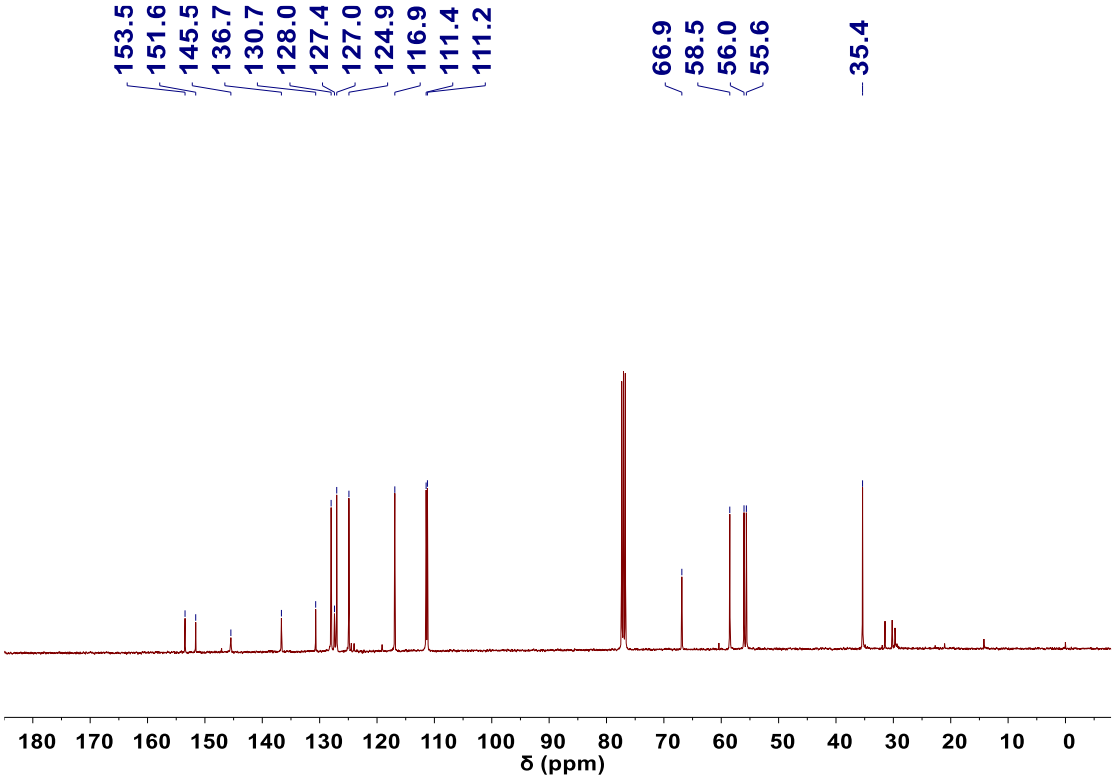

Fig. S2 ^{13}C NMR spectrum (100 MHz, $CDCl_3$, 298 K) of *rac*-**MTB**.

Synthesis of M[3] and characterization data

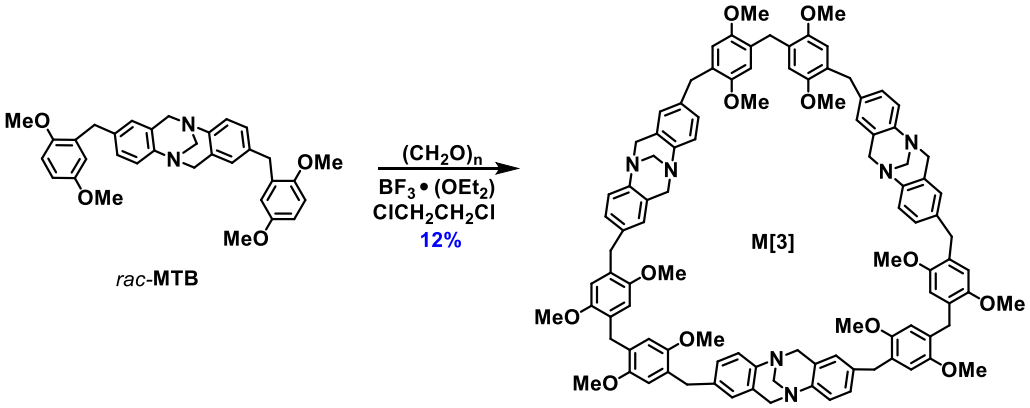

rac-**MTB** (0.20 g, 0.4 mmol) and paraformaldehyde (0.040 g, 1.2 mmol), 60 mL of 1,2-dichloroethane were added to a 100 mL round-bottom flask. $BF_3{\cdot}O(C_2H_5)_2$ (0.4 mL, 3.1 mmol) was added to the solution and the mixture was stirred at room temperature for 1 h. The reaction was quenched with $NaHCO_3$ solution. The organic layer was dried over anhydrous Na_2SO_4 and concentrated. Then the solvent was concentrated by rotary evaporation. The residue was purified by column chromatography on silica gel (eluent: 50/1, v/v, dichloromethane : methano) to afford **M[3]** (0.025 g, 12%), as a yellow solid. Elemental analysis: C 76.67%, H 6.68%, N 5.46%), corresponding to $C_{102}H_{102}N_6O_{12}$ with the calculated (C 76.38%, H 6.41%, N 5.24%). ^{1}H NMR (400 MHz, $CDCl_3$) δ 7.01 (d, 12H), 6.70 (s, 6H), 6.63 (d, *J* = 1.7 Hz, 6H), 6.57 (d, *J* = 1.7 Hz, 6H), 4.63 (d, *J* = 16.7 Hz, 6H), 4.29 (s, 6H), 4.08 (d, *J* = 16.7 Hz, 6H), 3.88 (s, 6H), 3.82 (s, 12H), 3.68 (d, *J* = 1.8 Hz, 18H), 3.62 (d, *J* = 1.8 Hz, 18H). ^{13}C NMR (100 MHz, $CDCl_3$) δ 151.5, 151.2, 145.6, 136.9, 127.9, 127.7, 127.5, 127.4, 126.8, 124.8, 113.9, 113.5, 67.0, 58.6, 56.1, 35.2, 29.8.

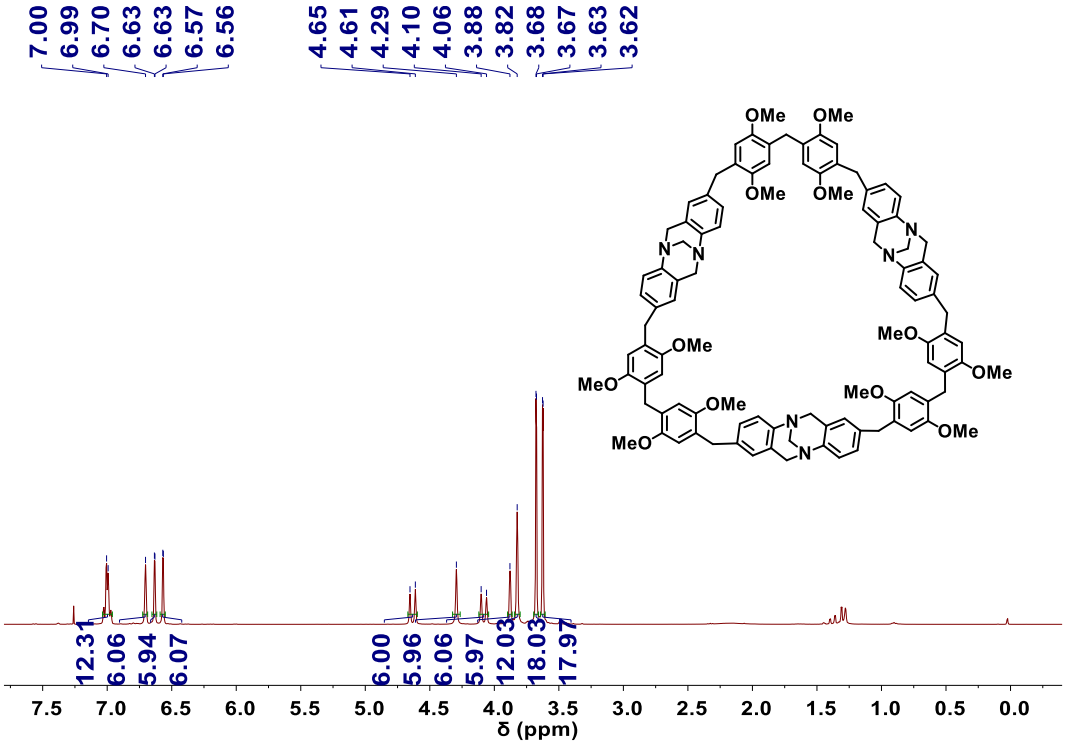

Fig. S3 ^{1}H NMR spectrum (400 MHz, $CDCl_3$, 298 K) of **M[3]**.

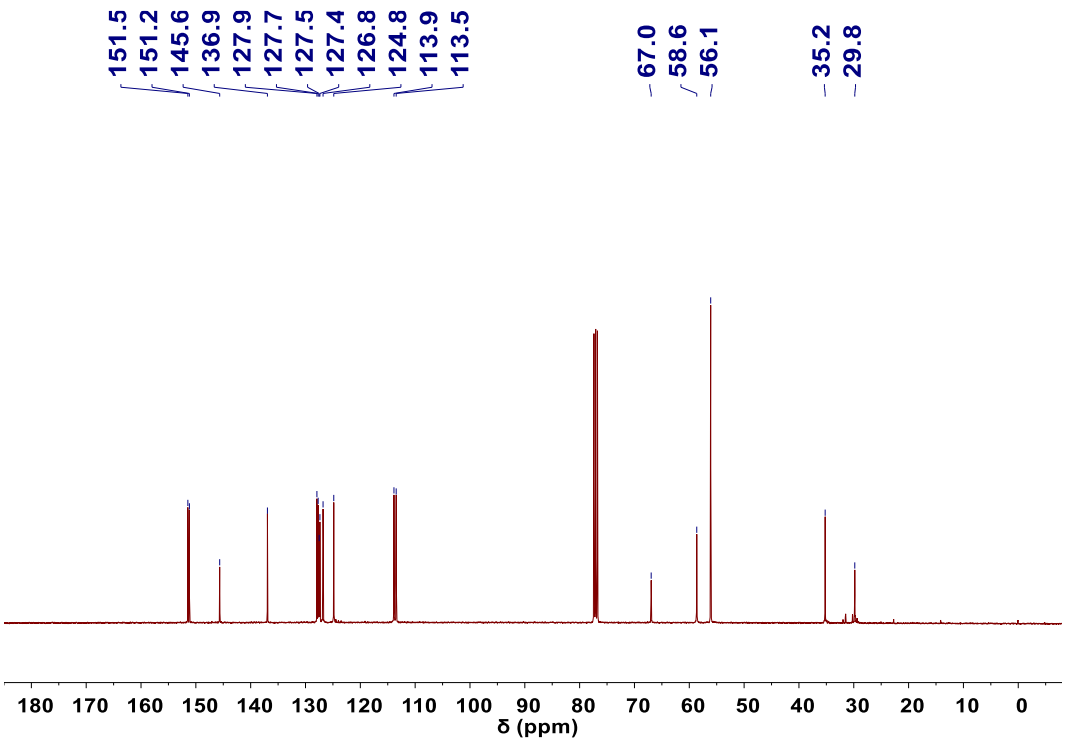

Fig. S4 ^{13}C NMR spectrum (100 MHz, $CDCl_3$, 298 K) of **M[3]**.

Synthesis of *rac*-ETB and characterization data

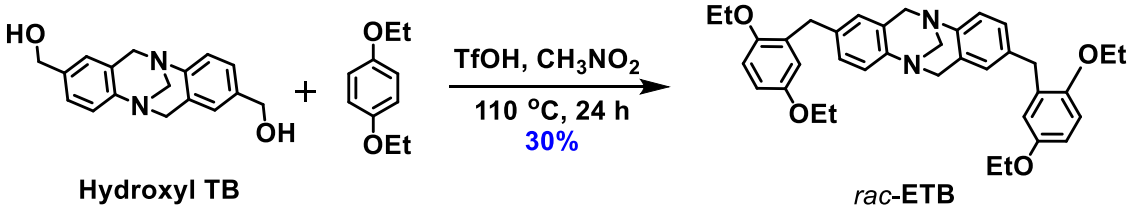

To the solution of **Hydroxyl TB** (1.00 g, 3.5 mmol) and 1,4-Diethoxybenzene (3.48 g, 21.2 mmol) in CH_3NO_2 (150 mL) was added trifluoromethanesulfonic acid (0.7 mL). The mixture was stirred at 110 °C for 24 h. Then the solvent was concentrated by rotary evaporation. The residue was purified by column chromatography on silica gel (eluent: 3/1, v/v, dichloromethane : ethyl acetate) to afford *rac*-**ETB** (0.62 g, 30%), as a yellow solid. ^{1}H NMR (400 MHz, $CDCl_3$) δ 7.04 (s, 4H), 6.77 (s, 2H), 6.74 (s, 2H), 6.69 (d, *J* = 3.0 Hz, 2H), 6.67 (d, *J* = 3.0 Hz, 2H), 4.64 (d, *J* = 16.7 Hz, 2H), 4.30 (s, 2H), 4.11 (d, *J* = 16.7 Hz, 2H), 3.93 (d, *J* = 7.0 Hz, 8H), 3.82 (s, 4H), 1.36 (t, *J* = 7.0 Hz, 6H), 1.30 (t, *J* = 7.0 Hz, 6H).

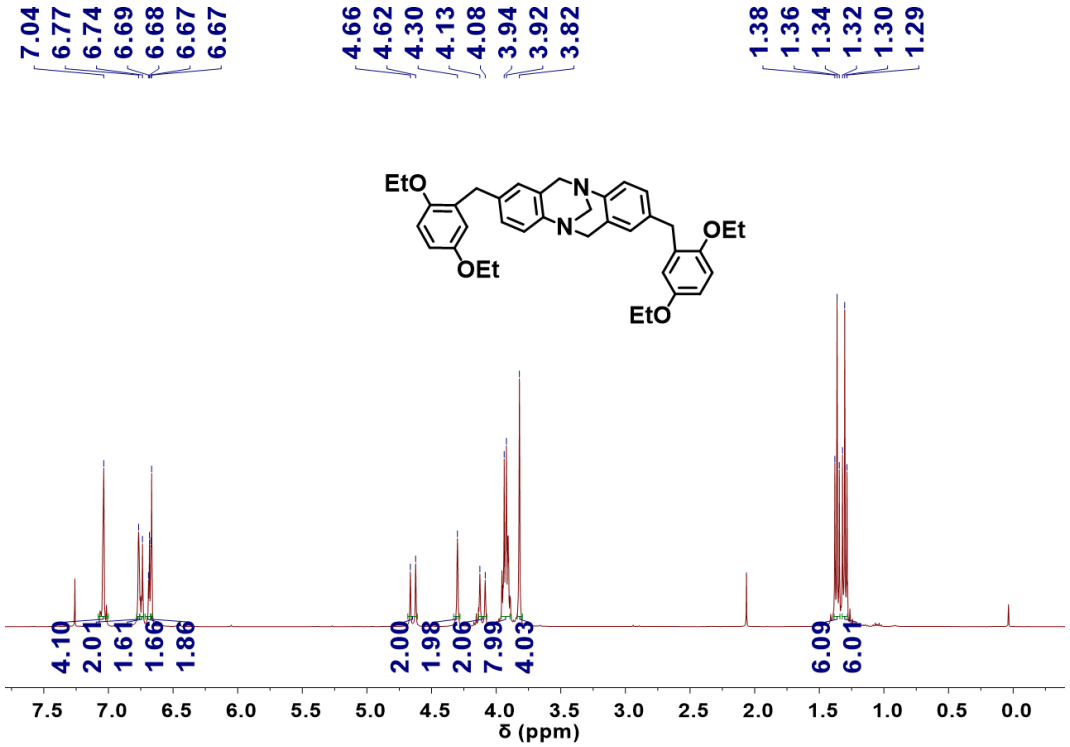

Fig. S5 ^{1}H NMR spectrum (400 MHz, $CDCl_3$, 298 K) of *rac*-**ETB**.

Characterization data of *R*$_{2N}$-ETB.

^{1}H NMR (500 MHz, $CDCl_3$) δ 7.02 (d, 4H), 6.75 (s, 2H), 6.73 (s, 2H), 6.67 (s, 2H), 6.65 (s, 2H), 4.63 (d, *J* = 16.7 Hz, 2H), 4.28 (s, 2H), 4.09 (d, *J* = 16.7 Hz, 2H), 3.92 (m , 8H), 3.80 (s, 4H), 1.35 (t, *J* = 7.0 Hz, 6H), 1.29 (t, *J* = 7.0 Hz, 6H). ^{13}C NMR (125 MHz, $CDCl_3$) δ 152.7, 150.8, 145.7, 136.7, 131.1, 128.0, 127.4, 127.1, 124.7, 117.3, 112.7, 111.9, 66.9, 64.3, 63.8, 58.6, 35.7, 14.9, 14.9. $[\alpha]_D^{25\,^{\circ}C}$ = −110.2 (1.0 × 10^{-2} g/mL, CH_2Cl_2).

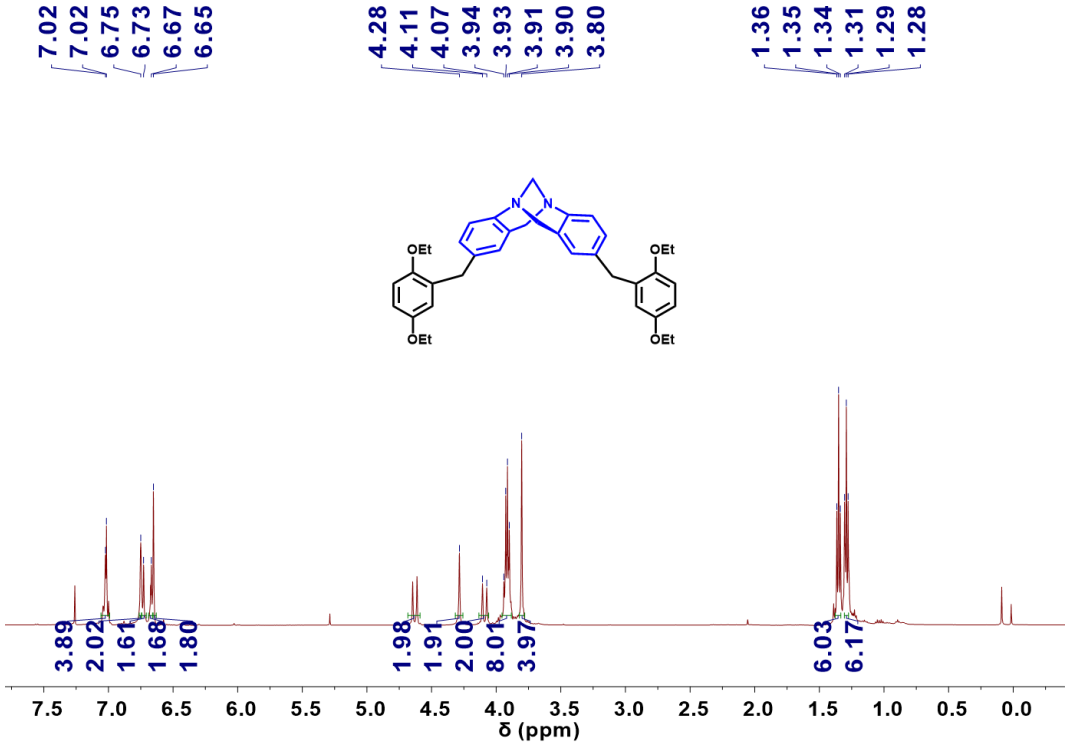

Fig. S6 ^{1}H NMR spectrum (500 MHz, $CDCl_3$, 298 K) of R_{2N}-**ETB**.

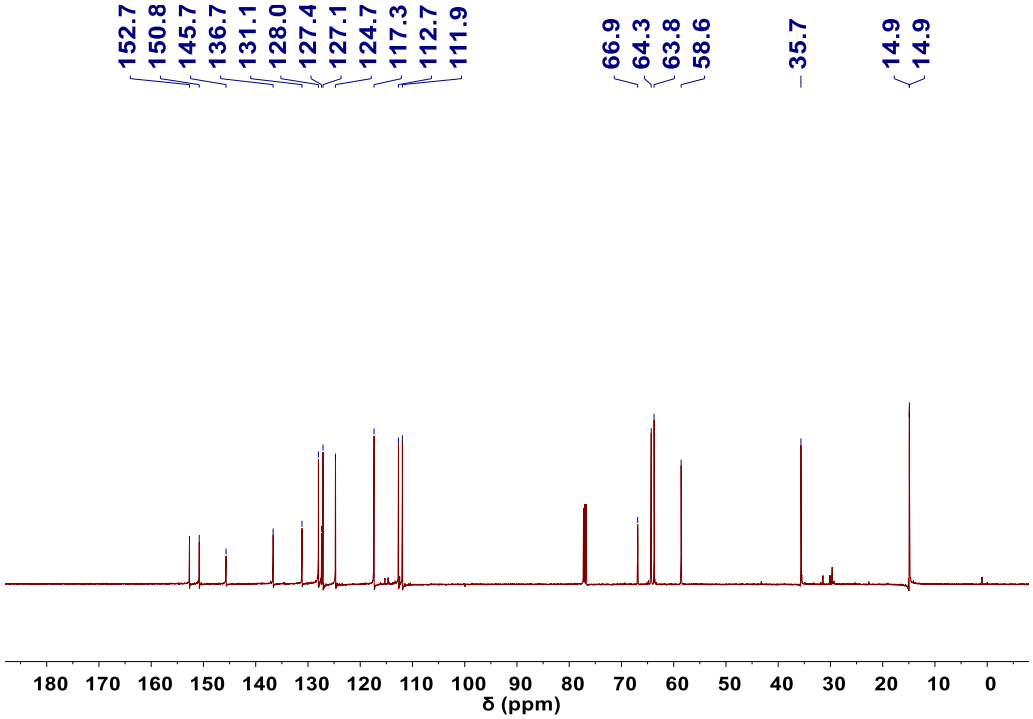

Fig. S7 ^{13}C NMR spectrum (125 MHz, $CDCl_3$, 298 K) of R_{2N}-**ETB**.

Characterization data of S_{2N}-ETB.

^{1}H NMR (400 MHz, $CDCl_3$) δ 7.04 (d, 4H), 6.76 (s, 2H), 6.74 (s, 2H), 6.69 (d, J = 3.0 Hz, 2H), 6.67 (d, J = 3.0 Hz, 2H), 4.64 (d, J = 16.7 Hz, 2H), 4.30 (s, 2H), 4.11 (d, J = 16.7 Hz, 2H), 3.93 (d, J = 7.0 Hz, 8H), 3.82 (s, 4H), 1.36 (t, J = 7.0 Hz, 6H), 1.31 (t, J = 7.0 Hz, 6H).^{13}C NMR (125 MHz, $CDCl_3$) δ 152.7, 150.9, 145.8, 136.7, 131.2, 128.0, 127.5, 127.2, 124.8, 117.4, 112.7, 112.0, 67.0, 64.4, 63.8, 58.7, 35.7, 15.0, 15.0. $[\alpha]_D^{25\,℃}$ = +108.9 (1.0 × 10^{-2} g/mL, CH_2Cl_2).

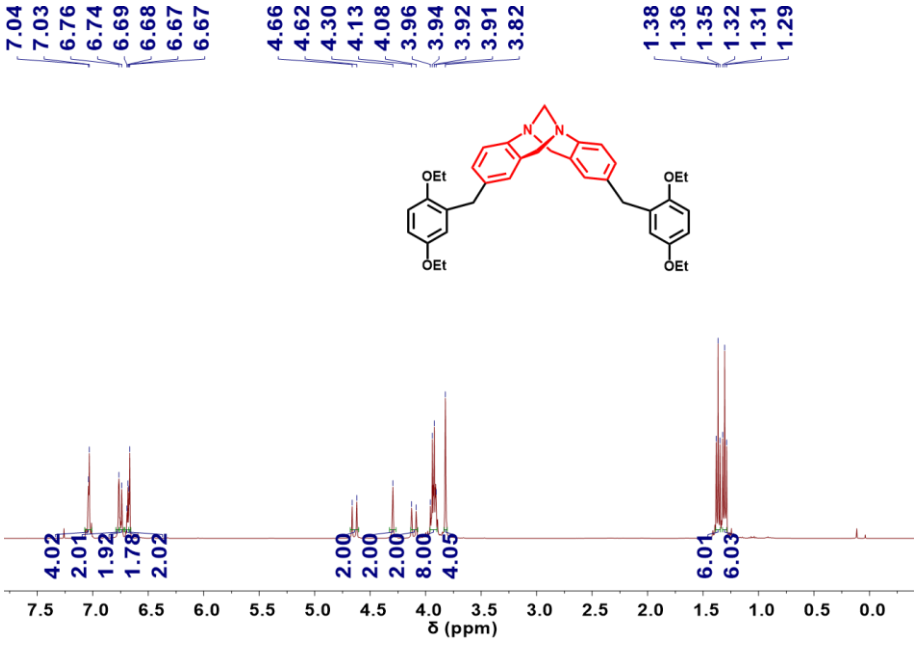

Fig. S8 ^{1}H NMR spectrum (400 MHz, $CDCl_3$, 298 K) of S_{2N}-**ETB**.

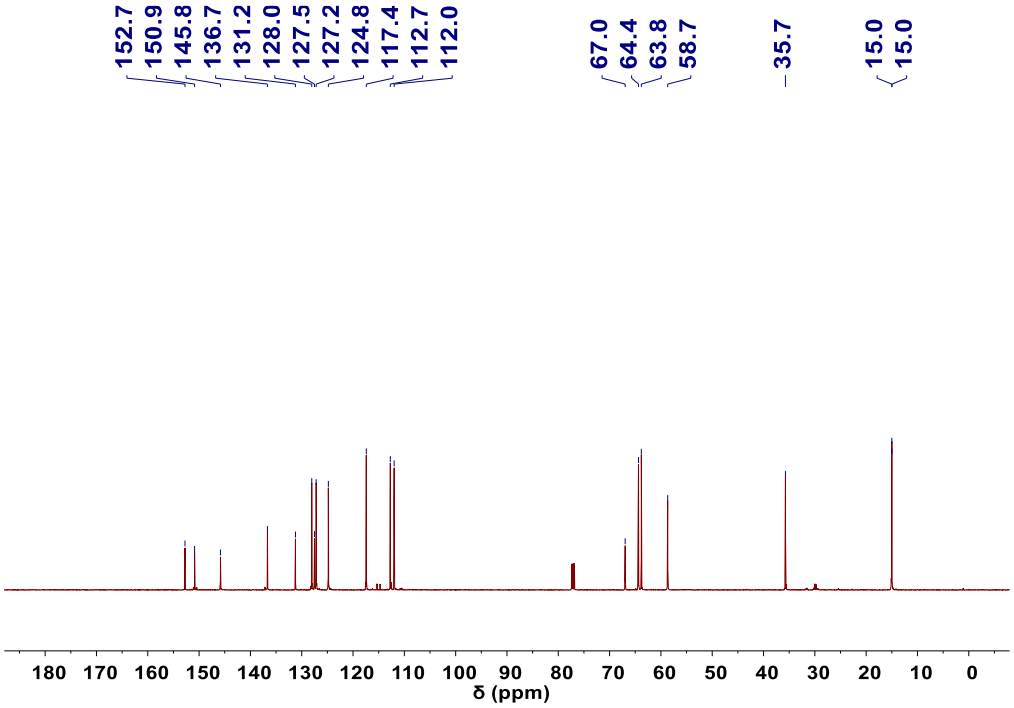

Fig. S9 ^{13}C NMR spectrum (125 MHz, $CDCl_3$, 298 K) of *S*$_{2N}$-**ETB**.

Synthesis of E[3] and characterization data

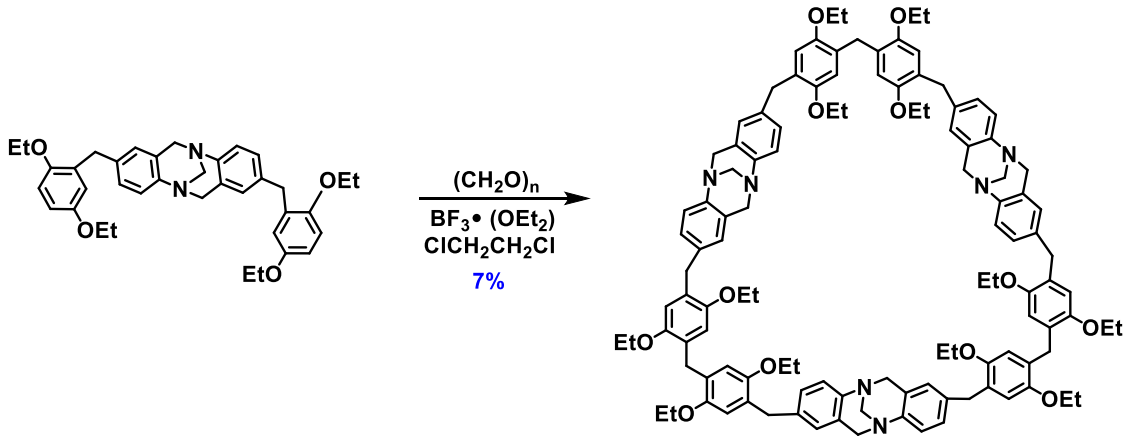

rac-**ETB** E[3]

rac-**ETB** (2.55 g, 4.4 mmol) and paraformaldehyde (0.40 g, 13.3 mmol), 500 mL of 1,2-dichloroethane were added to a 1000 mL round-bottom flask. $BF_3{\cdot}O(C_2H_5)_2$ (2.0 mL, 15.5 mmol) was added to the solution and the mixture was stirred at room temperature for 40 minutes. The reaction was quenched with $NaHCO_3$ solution. The organic layer was dried over anhydrous Na_2SO_4 and concentrated. Then the solvent was concentrated by rotary evaporation. The residue was purified by column chromatography on silica gel (eluent: 60/1, v/v, dichloromethane : methanol) to afford **E[3]** (0.20 g, 7%), as a yellow solid. Elemental analysis: C 77.48%, H 7.32%, N 4.52%, corresponding to $C_{114}H_{126}N_6O_{12}$ with the calculated (C 77.26%, H 7.17%, N 4.74%). ^{1}H NMR (400 MHz, $CDCl_3$) δ 7.00 (s, 12H), 6.72 (s, 6H), 6.68 (s, 6H), 6.57 (s, 6H), 4.63 (d, *J* = 16.7 Hz, 6H), 4.30 (s, 6H), 4.07 (d, *J* = 16.7 Hz, 6H), 3.91 – 3.77 (m, 42H), 1.31 (t, *J* = 6.9 Hz, 18H), 1.19 (t, *J* = 6.9 Hz, 18H). ^{13}C NMR (100 MHz, $CDCl_3$) δ 150.7, 150.3, 145.2, 137.4, 128.5, 127.8, 127.7, 127.2, 126.9, 124.6, 115.3, 114.6, 67.0, 64.4, 64.3, 58.6, 35.5, 29.9, 15.1, 14.9.

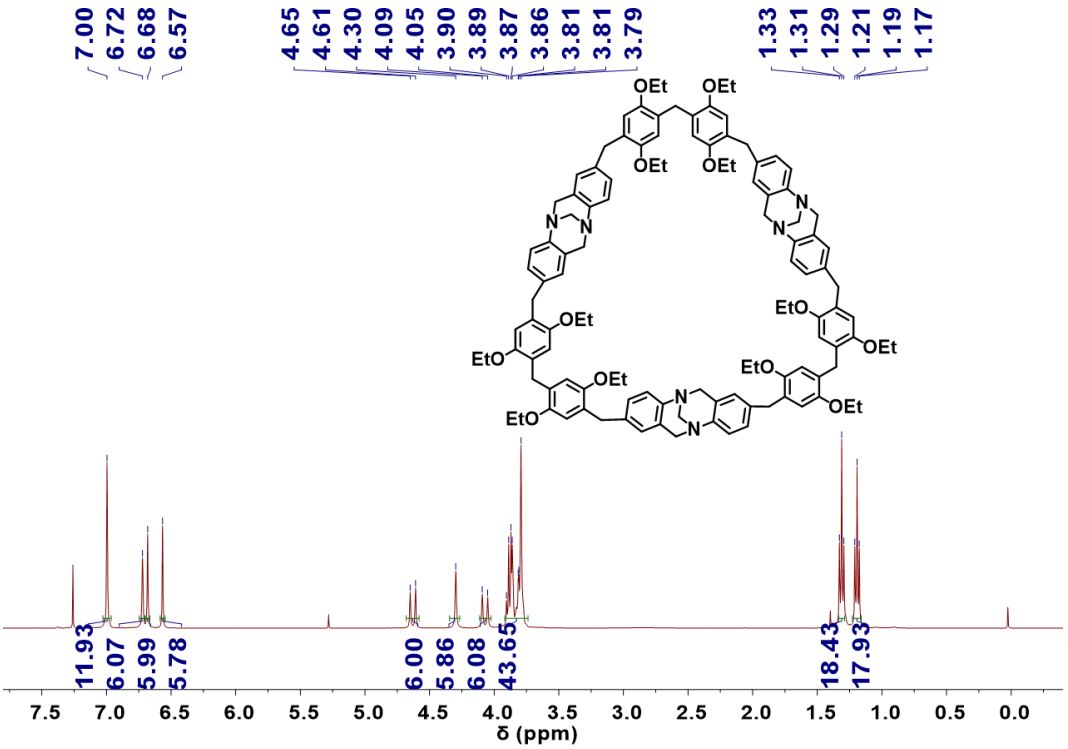

Fig. S10 ^{1}H NMR spectrum (400 MHz, $CDCl_3$, 298 K) of **E[3]**.

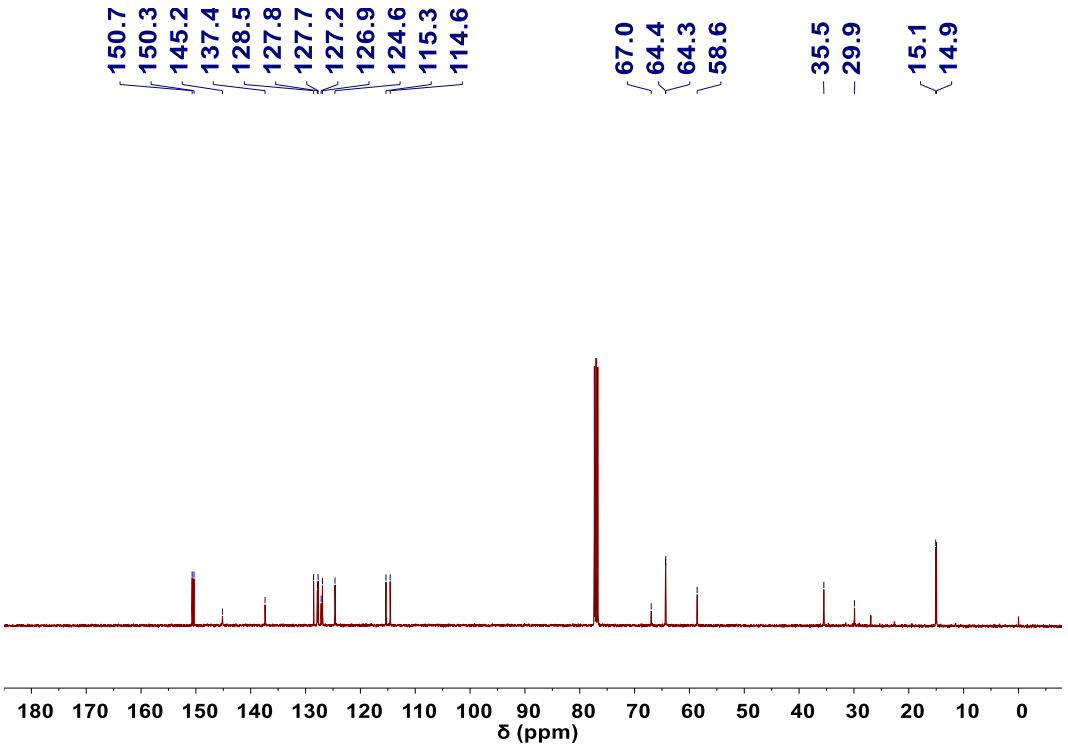

Fig. S11 ^{13}C NMR spectrum (100 MHz, $CDCl_3$, 298 K) of **E[3]**.

Synthesis of *rac*-BTB and characterization data

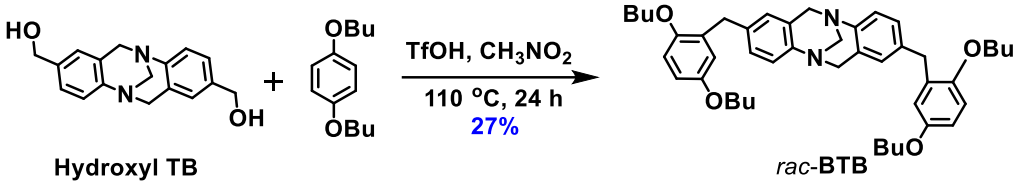

To the solution of **Hydroxyl TB** (0.30 g, 1.0 mmol) and 1,4-Dibutoxybenzene (1.36 g, 6.1 mmol) in CH_3NO_2 (25 mL) was added trifluoromethanesulfonic acid (0.2 mL). The mixture was stirred at 110 °C for 24 h. Then the solvent was concentrated by rotary evaporation. The residue was purified by column chromatography on silica gel (eluent: 3/1, v/v, dichloromethane : ethyl acetate) to afford *rac*-**BTB** (0.20 g, 27%), as a yellow solid. ^{1}H NMR (400 MHz, $CDCl_3$) δ 7.02 (s, 4H), 6.75 (s, 2H), 6.73 (s, 2H), 6.68 (d, *J* = 3.0 Hz, 2H), 6.66 (d, *J* = 3.0 Hz, 2H), 4.63 (d, *J* = 16.7 Hz, 2H), 4.29 (s, 2H), 4.09 (d, *J* = 16.7 Hz, 2H), 3.85 (td, *J* = 6.4, 2.3 Hz, 8H), 3.81 (s, 4H), 1.68 (m, 8H), 1.43 (m, 8H), 0.93 (m, 12H). ^{13}C NMR (125 MHz, $CDCl_3$) δ 152.9, 150.9, 142.4, 138.9, 130.4, 128. 8, 127.2, 125.9, 124.5, 117.6, 112.4, 112.2, 68.3, 68.2, 67.3, 58.1, 35.8, 31.5, 19.3, 13.9, 13.9.

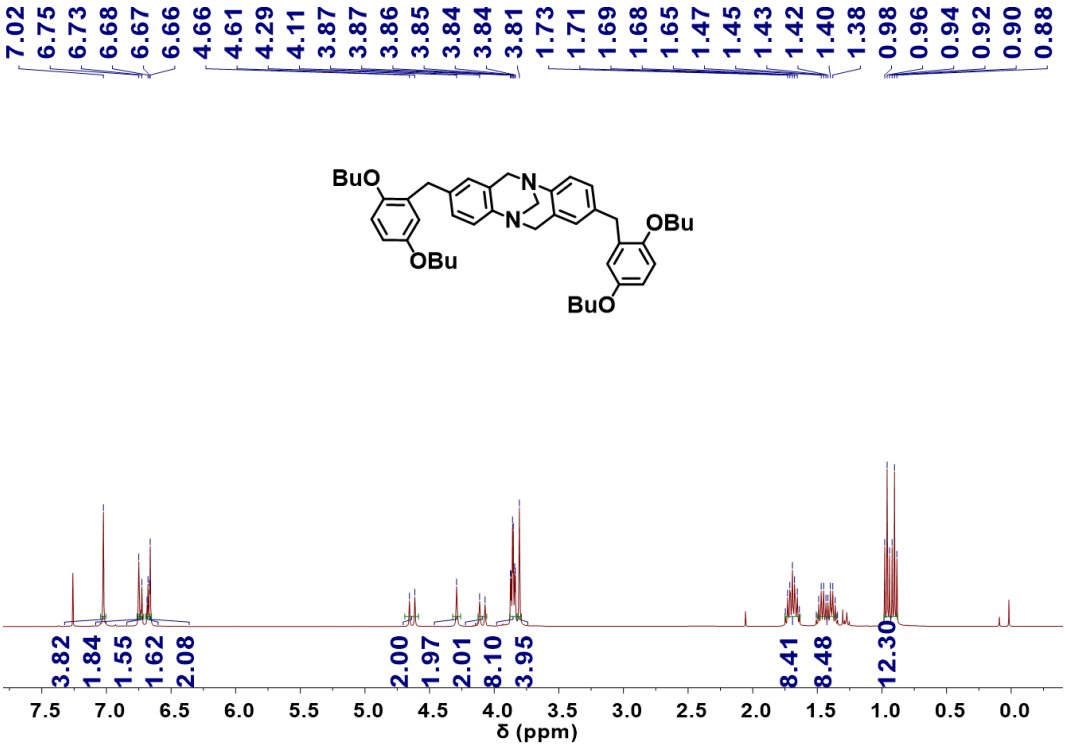

Fig. S12 ^{1}H NMR spectrum (400 MHz, $CDCl_3$, 298 K) of *rac*-**BTB**.

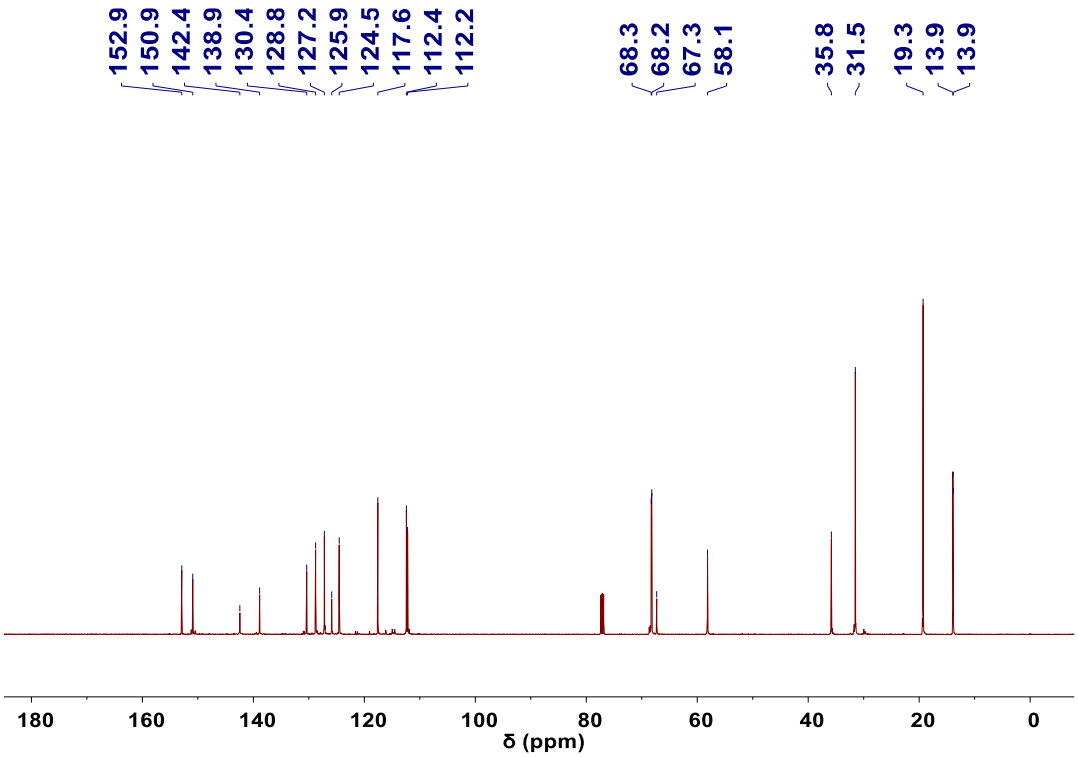

Fig. S13 ^{13}C NMR spectrum (125 MHz, $CDCl_3$, 298 K) of *rac*-**BTB**.

Synthesis of B[3] and characterization data

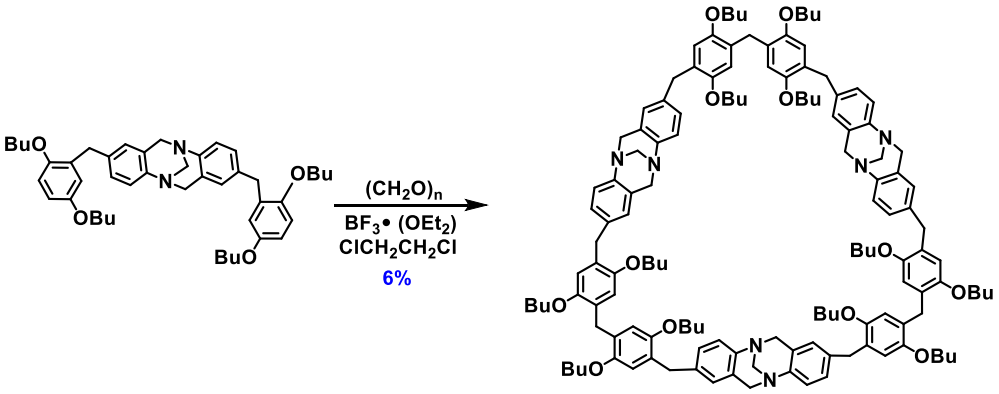

rac-**BTB** B[3]

rac-**BTB** (1.90 g, 2.7 mmol) and paraformaldehyde (0.25 g, 8.2 mmol), 400 mL of 1,2-dichloroethane were added to a 1000 mL round-bottom flask. $BF_3{\cdot}O(C_2H_5)_2$ (2.0 mL, 15.5 mmol) was added to the solution and the mixture was stirred at room temperature for 20 minutes. The reaction was quenched with $NaHCO_3$ solution. The organic layer was dried over anhydrous Na_2SO_4 and concentrated. Then the solvent was concentrated by rotary evaporation. The residue was purified by column chromatography on silica gel (eluent: 60/1, v/v, dichloromethane : methanol) to afford **B[3]** (0.32 g, 6%), as a yellow solid. Elemental analysis: C 78.30%, H 8.52%, N 3.76%, corresponding to $C_{138}H_{174}N_6O_{12}$ with the calculated (C 78.59%, H 8.32%, N 3.99%). ^{1}H NMR (500 MHz, $CDCl_3$) δ 7.00 (s, 12H), 6.72 (s, 6H), 6.68 (s, 6H), 6.58 (s, 6H), 4.63 (d, *J* = 16.7 Hz, 6H), 4.30 (s, 6H), 4.07 (d, *J* = 16.7 Hz, 6H), 3.87 (s, 6H), 3.83 (t, *J* = 6.4 Hz, 12H), 3.79 (s, 12H), 3.75 (t, *J* = 6.4 Hz, 12H), 1.73 – 1.66 (m, 12H), 1.62 – 1.55 (m, 12H), 1.47 – 1.40 (m, 12H), 1.34 – 1.28 (m, 12H), 0.91 (t, *J* = 7.4 Hz, 18H), 0.84 (t, *J* = 7.4 Hz, 18H). ^{13}C NMR (125 MHz, $CDCl_3$) δ 150.7, 150.4, 145.2, 137.5, 128.5, 127.8, 127.5, 127.1, 126.9, 124.7, 115.0, 114.4,

68.5, 68.3, 66.9, 58.5, 35.6, 31.7, 31.5, 29.8, 19.4, 19.2, 13.9, 13.8.

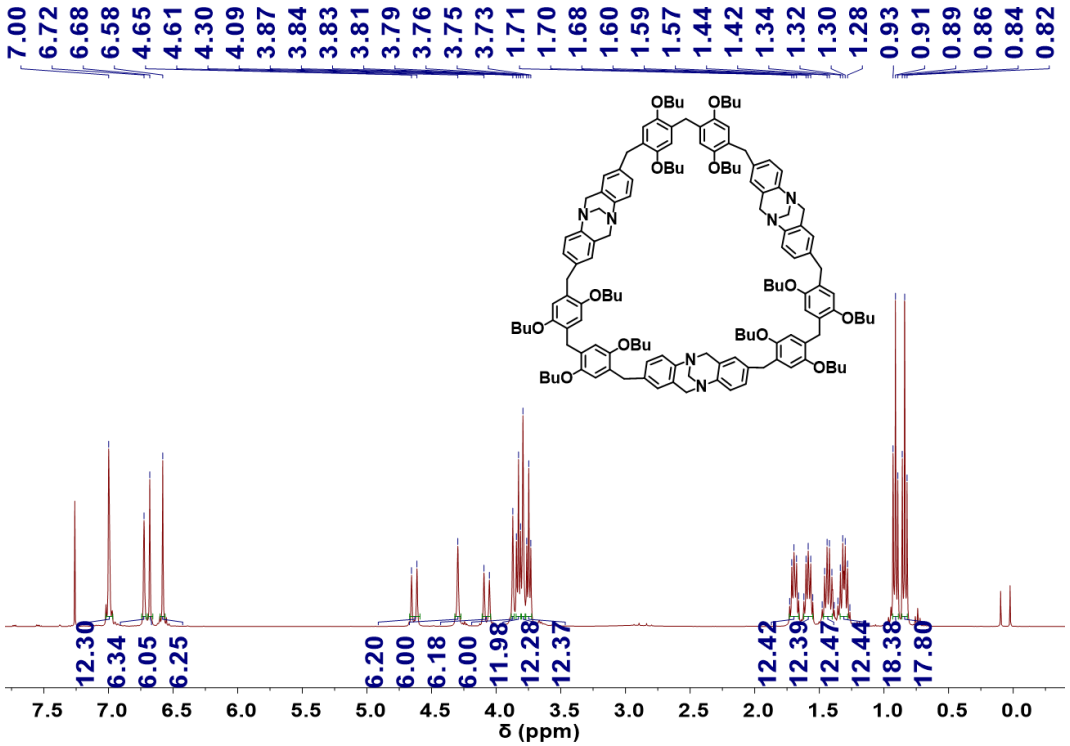

Fig. S14 ^{1}H NMR spectrum (500 MHz, $CDCl_3$, 298 K) of **B[3]**.

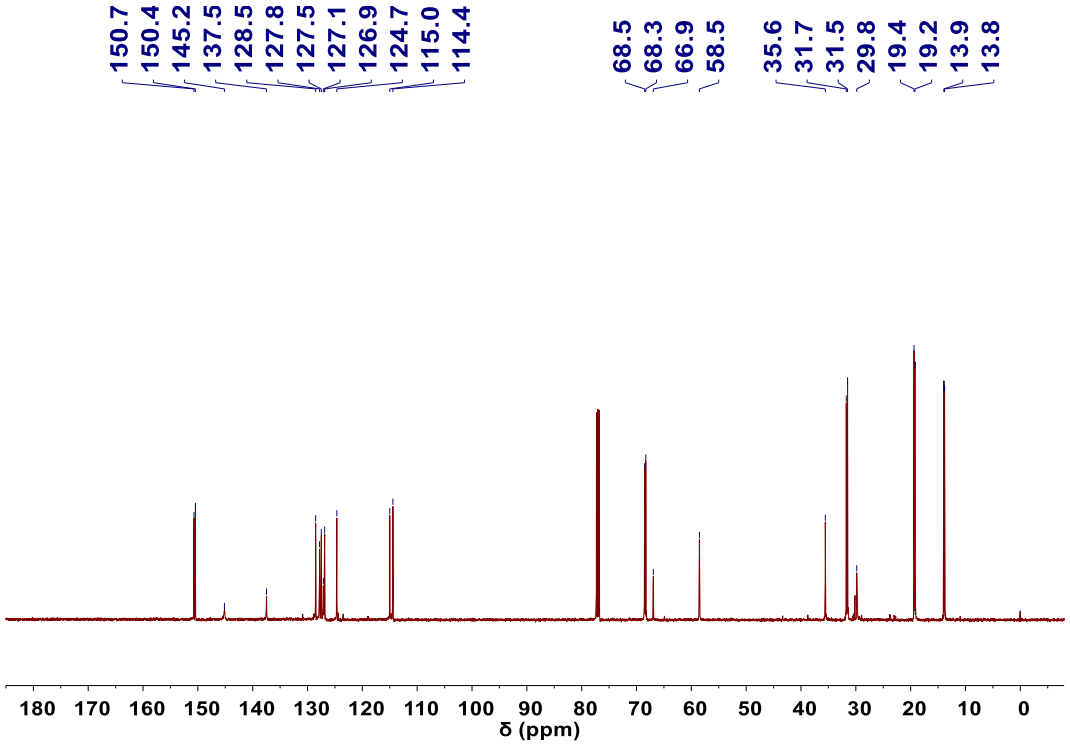

Fig. S15 ^{13}C NMR spectrum (125 MHz, $CDCl_3$, 298 K) of **B[3]**.

Synthesis of R_{6N}-E[3] and characterization data

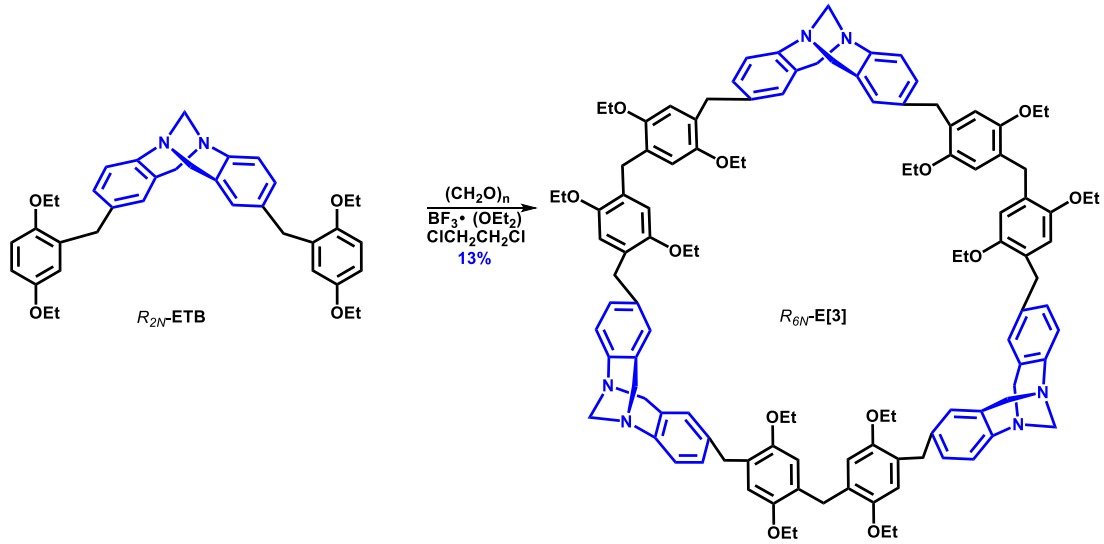

R_{2N}-**ETB** (0.19 g, 0.32 mmol) and paraformaldehyde (0.030 g, 1.0 mmol), 50 mL of 1,2-dichloroethane were added to a 100 mL round-bottom flask. $BF_3{\cdot}O(C_2H_5)_2$ (0.4 mL, 3.1 mmol) was added to the solution and the mixture was stirred at room temperature for 40 minutes. The reaction was quenched with $NaHCO_3$ solution. The organic layer was dried over anhydrous Na_2SO_4 and concentrated. Then the solvent was concentrated by rotary evaporation. The residue was purified by column chromatography on silica gel (eluent: 60/1, v/v, dichloromethane : methanol) to afford R_{6N}-**E[3]** (0.026 g, 13%), as a yellow solid. ^{1}H NMR (400 MHz, $CDCl_3$) δ 6.96 (s, 12H), 6.69 (s, 6H), 6.65 (s, 6H), 6.54 (s, 6H), 4.60 (d, J = 16.7 Hz, 6H), 4.26 (s, 6H), 4.04 (d, J = 16.7 Hz, 6H), 3.88 – 3.75 (m, 42H), 1.29 (t, J = 6.9 Hz, 18H), 1.16 (t, J = 6.9 Hz, 18H). ^{13}C NMR (100 MHz, $CDCl_3$) δ 150.7, 150.4, 145.6, 137.2, 128.5, 127.8, 127.8, 127.4, 126.9, 124.7, 115.4, 114.6, 67.0, 64.4, 64.4, 58.7, 35.5, 29.7, 15.1, 15.0. $[\alpha]_D^{25\,℃}$ = −59.1 (2.0 × 10^{-2} g/mL, CH_2Cl_2).

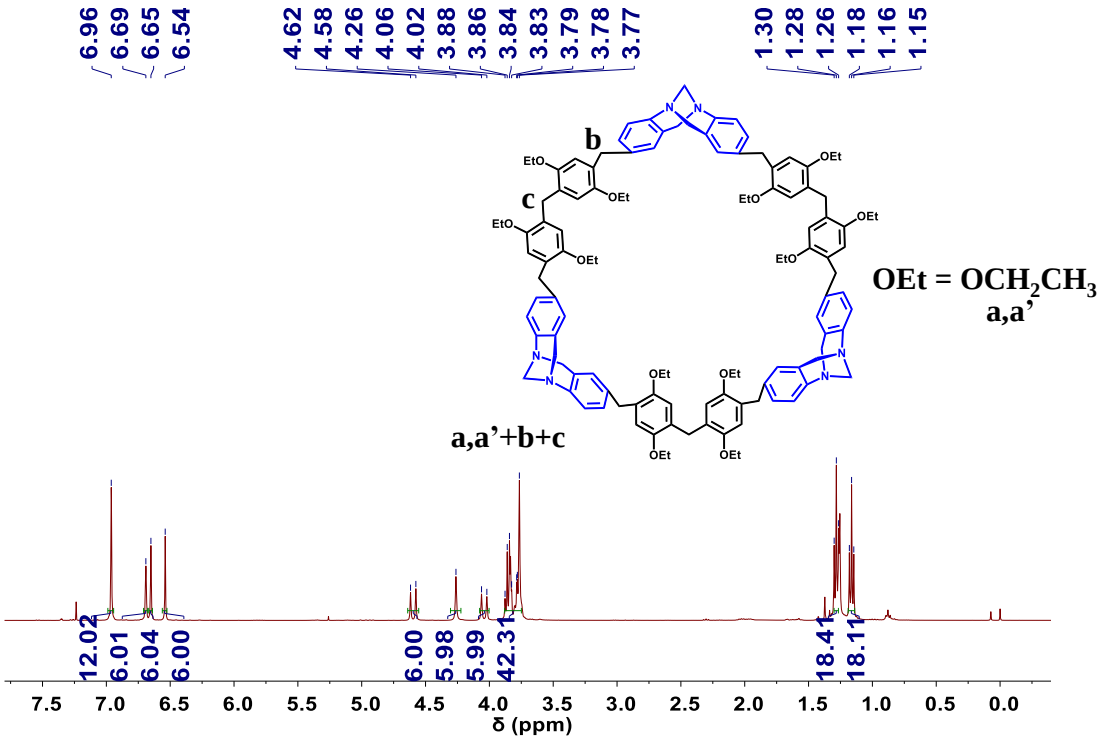

Fig. S16 ^{1}H NMR spectrum (400 MHz, $CDCl_3$, 298 K) of R_{6N}-**E[3]**.

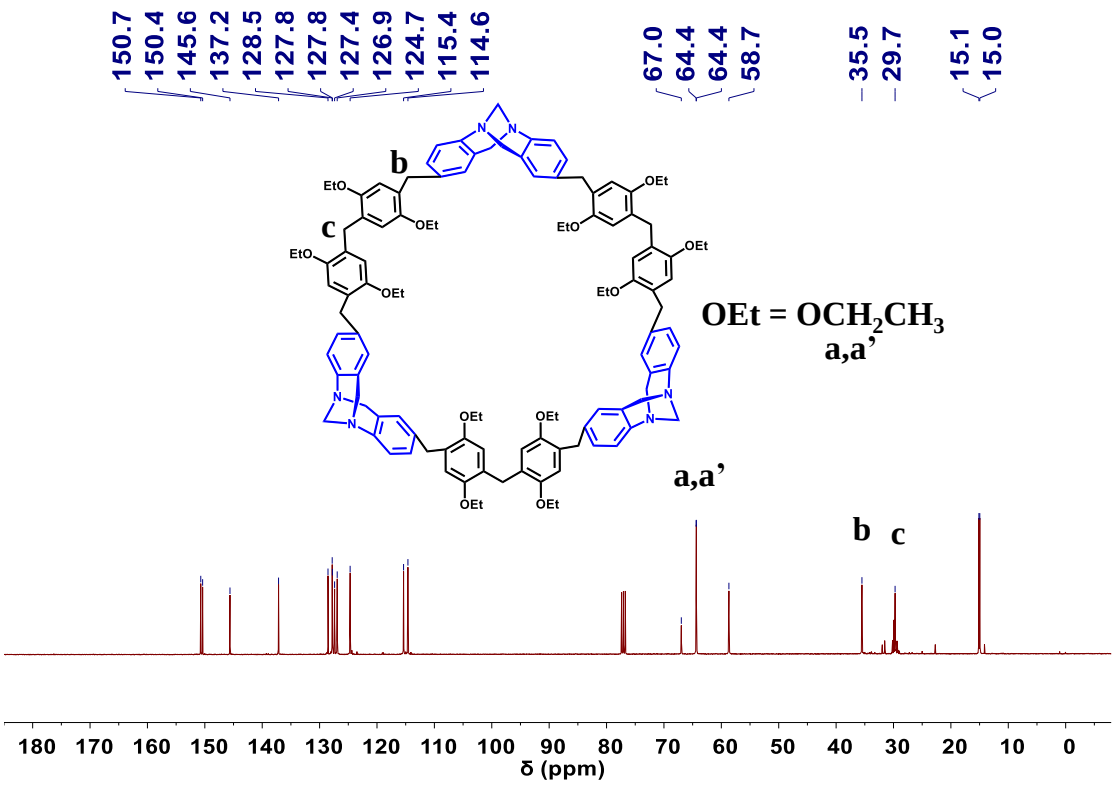

Fig. S17 ^{13}C NMR spectrum (100 MHz, $CDCl_3$, 298 K) of R_{6N}-**E[3]**.

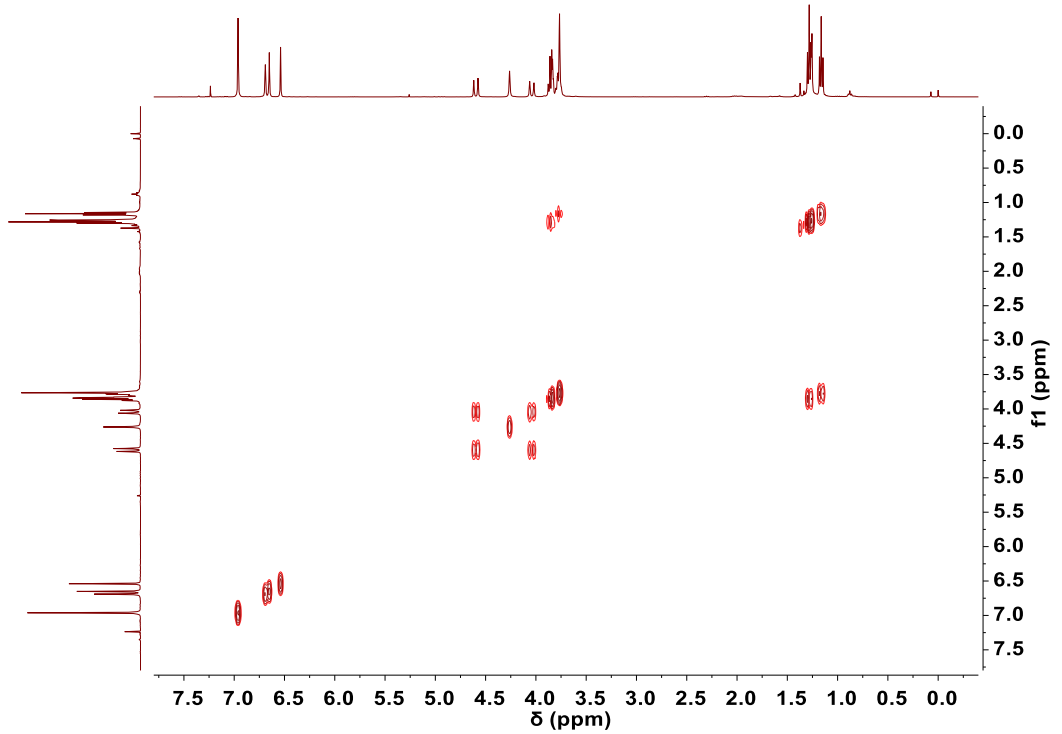

Fig. S18 ^{1}H-^{1}H COSY spectrum (400 MHz, $CDCl_3$, 298 K) of R_{6N}-**E[3]**.

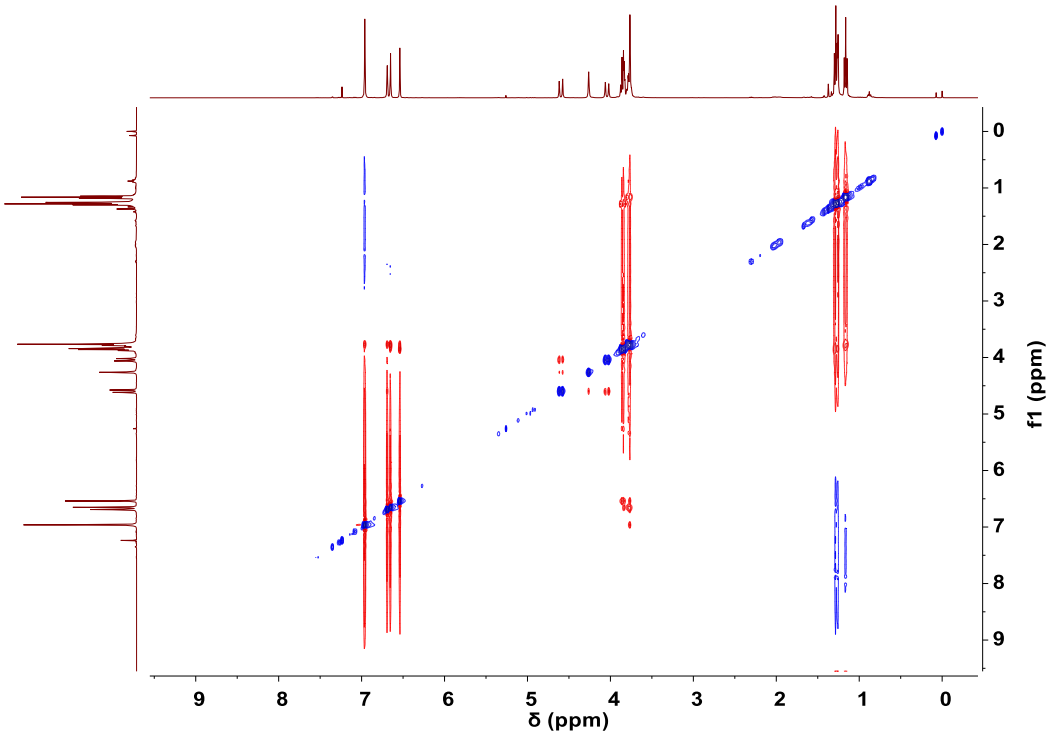

Fig. S19 ^{1}H-^{1}H NOESY spectrum (400 MHz, $CDCl_3$, 298 K) of *R*$_{6N}$-**E[3]**.

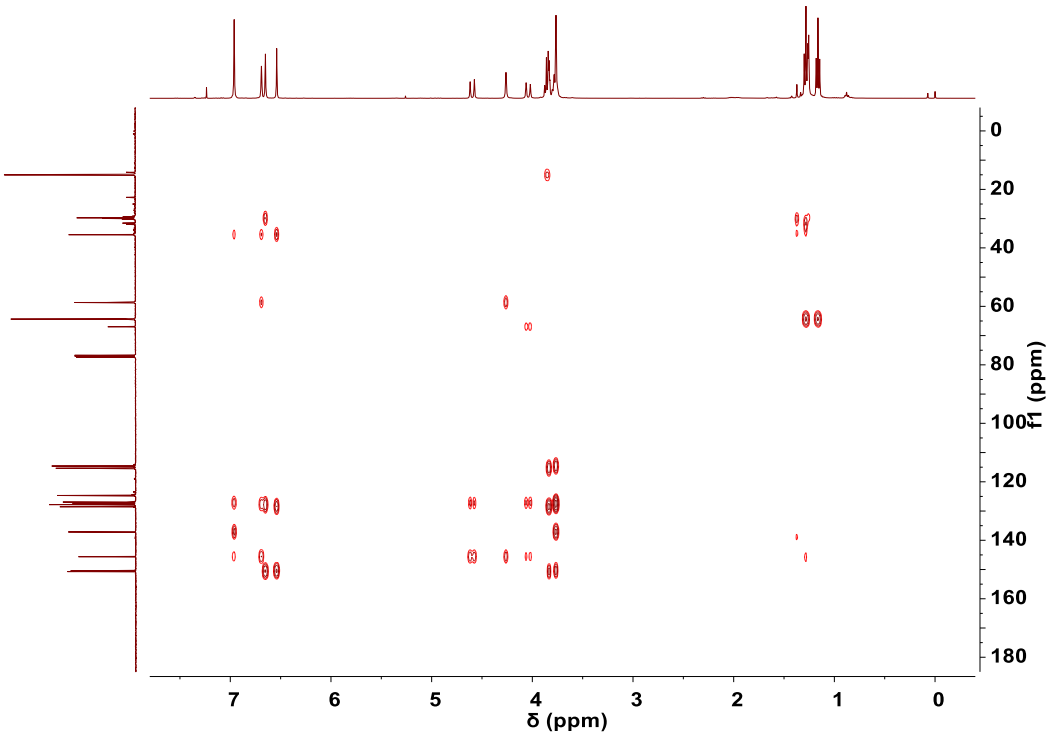

Fig. S20 HMBC NMR spectrum (100 MHz, $CDCl_3$, 298 K) of *R*$_{6N}$-**E[3]**.

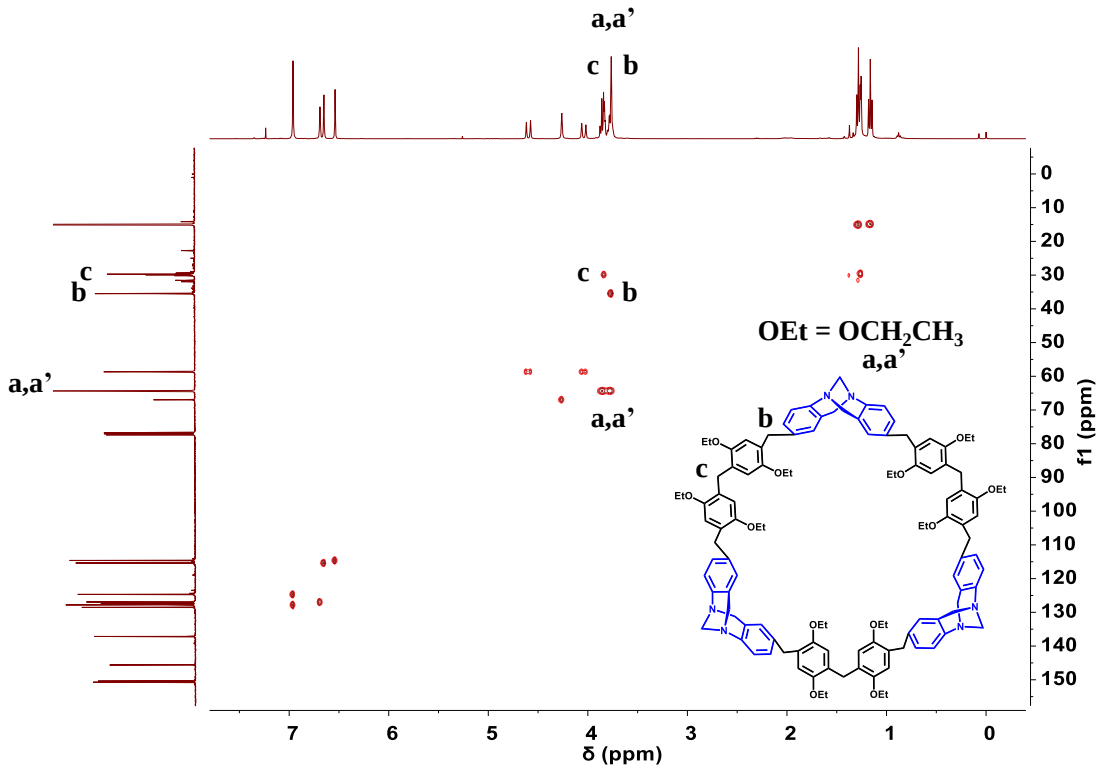

Fig. S21 HSQC NMR spectrum (100MHz, $CDCl_3$, 298 K) of R_{6N}-**E[3]**.

Synthesis of S_{6N}-E[3] and characterization data

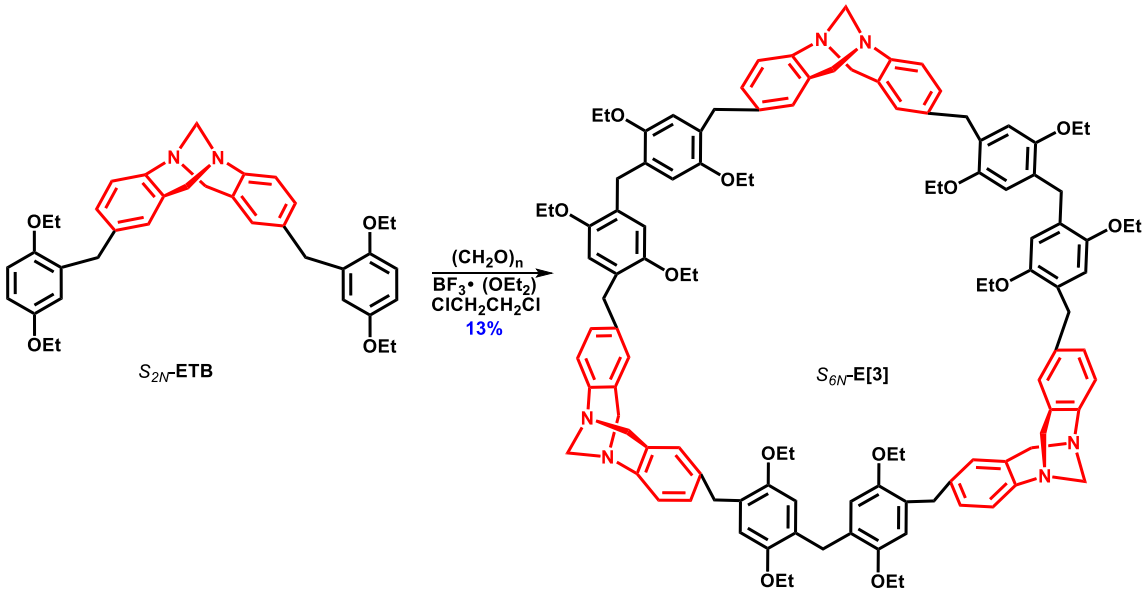

S_{2N} -**ETB** ((0.19 g, 0.32 mmol) and paraformaldehyde (0.03 g, 1.0 mmol), 50 mL of 1,2-dichloroethane were added to a 100 mL round-bottom flask. $BF_3{\cdot}O(C_2H_5)_2$ (0.4 mL, 3.1 mmol) was added to the solution and the mixture was stirred at room temperature for 40 minutes. The reaction was quenched with $NaHCO_3$ solution. The organic layer was dried over anhydrous Na_2SO_4 and concentrated. Then the solvent was concentrated by rotary evaporation. The residue was purified by column chromatography on silica gel (eluent: 60/1, v/v, dichloromethane : methanol) to afford S_{6N}-**E[3]** (0.024 g, 13%), as a yellow

solid. ^{1}H NMR (400 MHz, $CDCl_3$) δ 6.96 (s, 12H), 6.69 (s, 6H), 6.65 (s, 6H), 6.54 (s, 6H), 4.60 (d, *J* = 16.6 Hz, 6H), 4.26 (s, 6H), 4.04 (d, *J* = 16.7 Hz, 6H), 3.88 – 3.75 (m, 42H), 1.28 (t, *J* = 7.0 Hz, 32H), 1.16 (t, *J* = 7.0 Hz, 18H). ^{13}C NMR (100 MHz, $CDCl_3$) δ 150.7, 150.4, 145.6, 137.1, 128.5, 127.8, 127.7, 127.4, 126.9, 124.7, 115.3, 114.6, 67.0, 64.4, 64.3, 58.7, 35.5, 29.7, 15.1, 14.9. $[\alpha]_D^{25\,^{\circ}C}$ = +58.9 (2.0 × 10^{-2} g/mL, CH_2Cl_2).

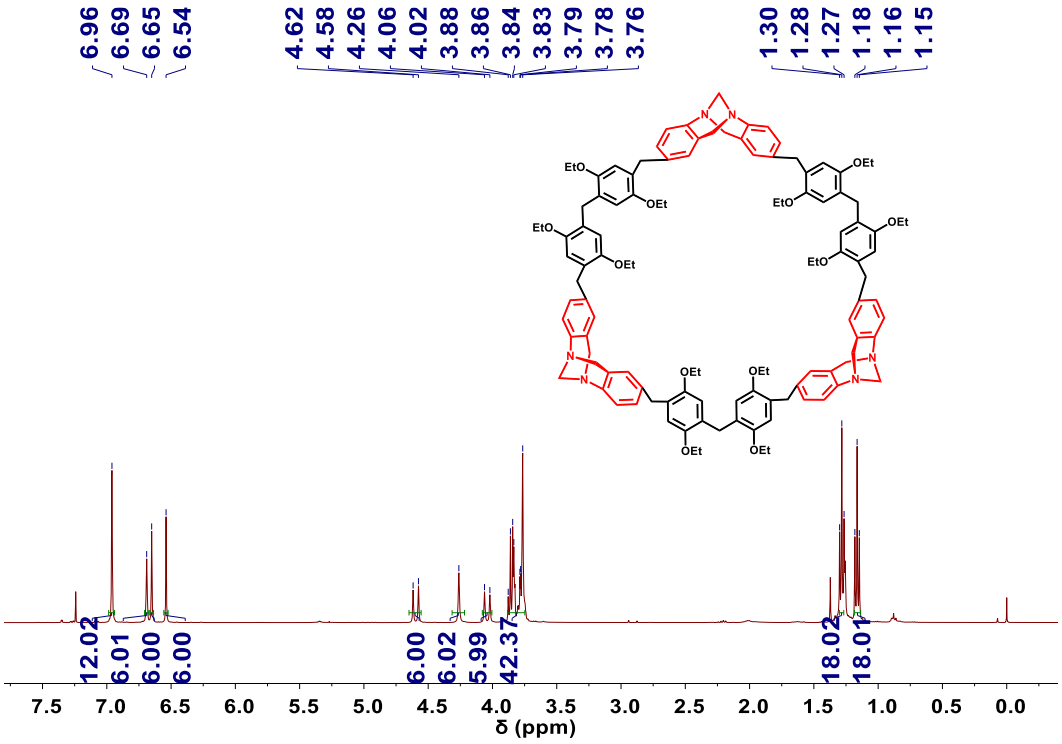

Fig. S22 ^{1}H NMR spectrum (400 MHz, $CDCl_3$, 298 K) of S_{6N}-**E[3]**.

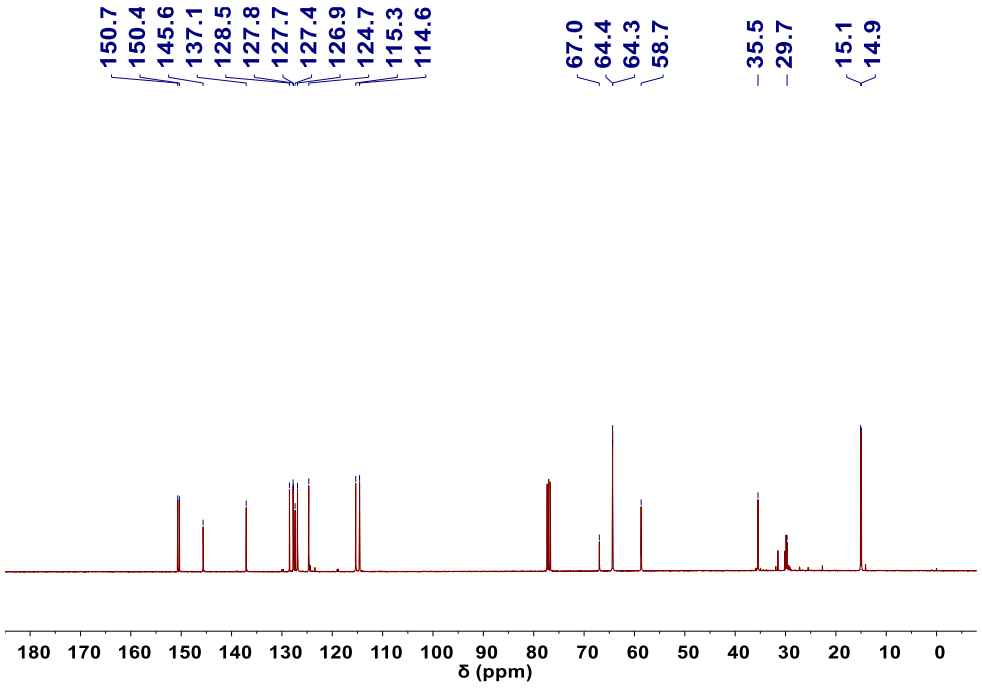

Fig. S23 ^{13}C NMR spectrum (100 MHz, $CDCl_3$, 298 K) of S_{6N}-**E[3]**.

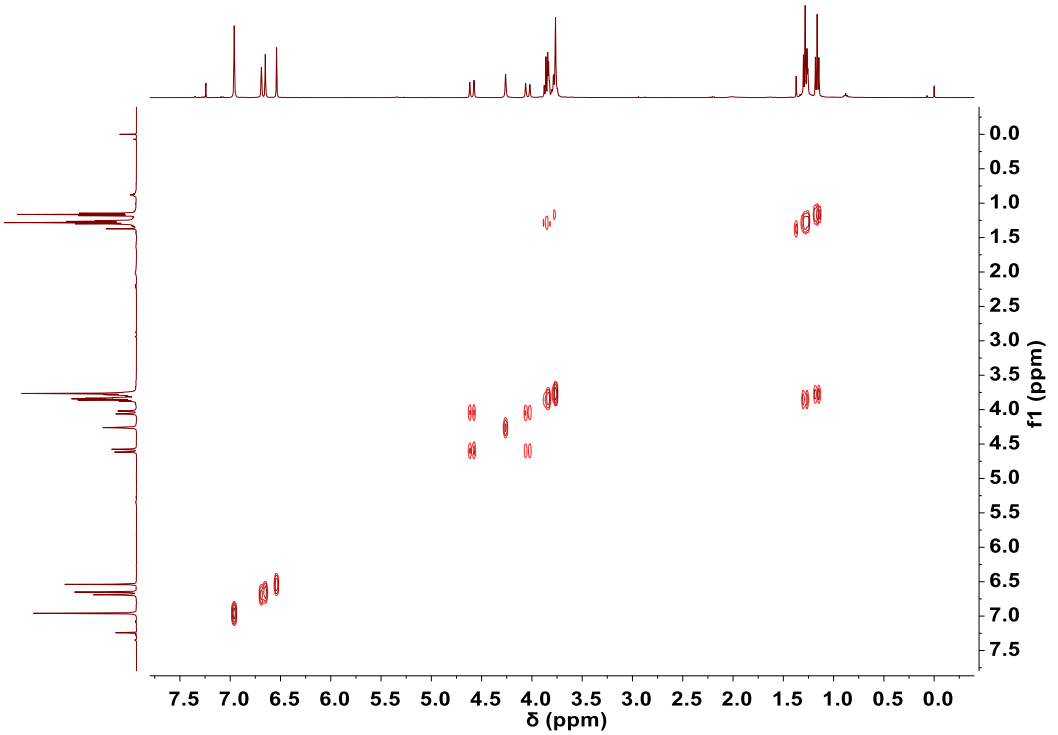

Fig. S24 ^{1}H-^{1}H COSY spectrum (400 MHz, $CDCl_3$, 298 K) of *S*$_{6N}$-**E[3]**.

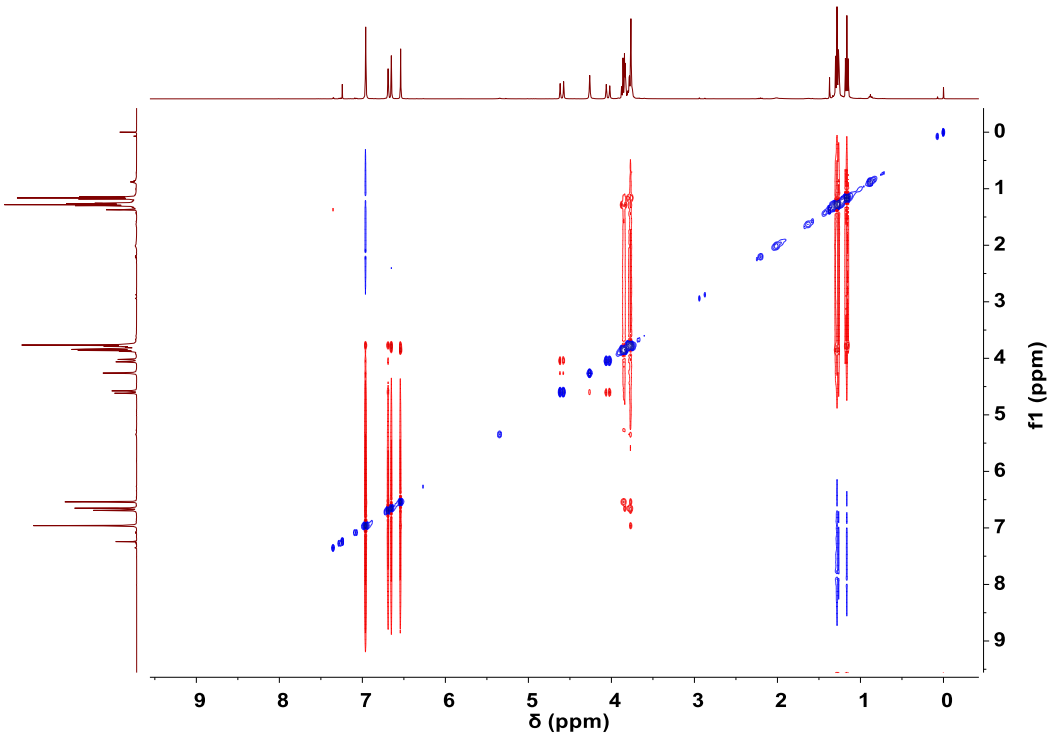

Fig. S25 ^{1}H-^{1}H NOESY spectrum (400 MHz, $CDCl_3$, 298 K) of *S*$_{6N}$-**E[3]**.

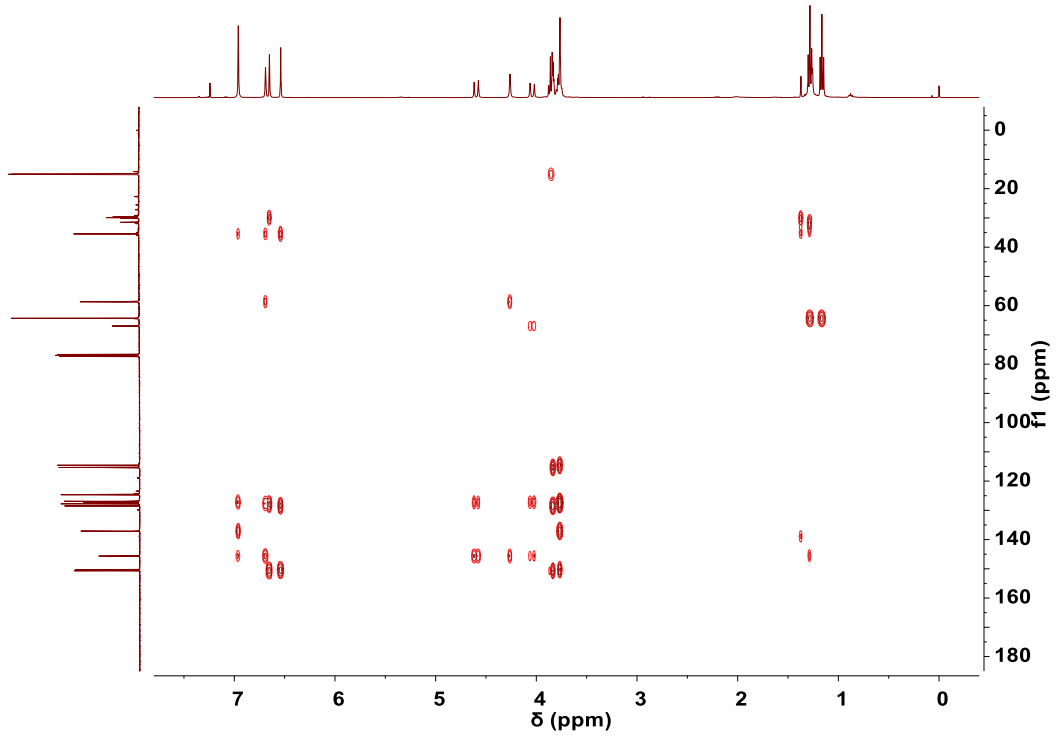

Fig. S26 HMBC NMR spectrum (100MHz, $CDCl_3$, 298 K) of S_{6N}-**E[3]**.

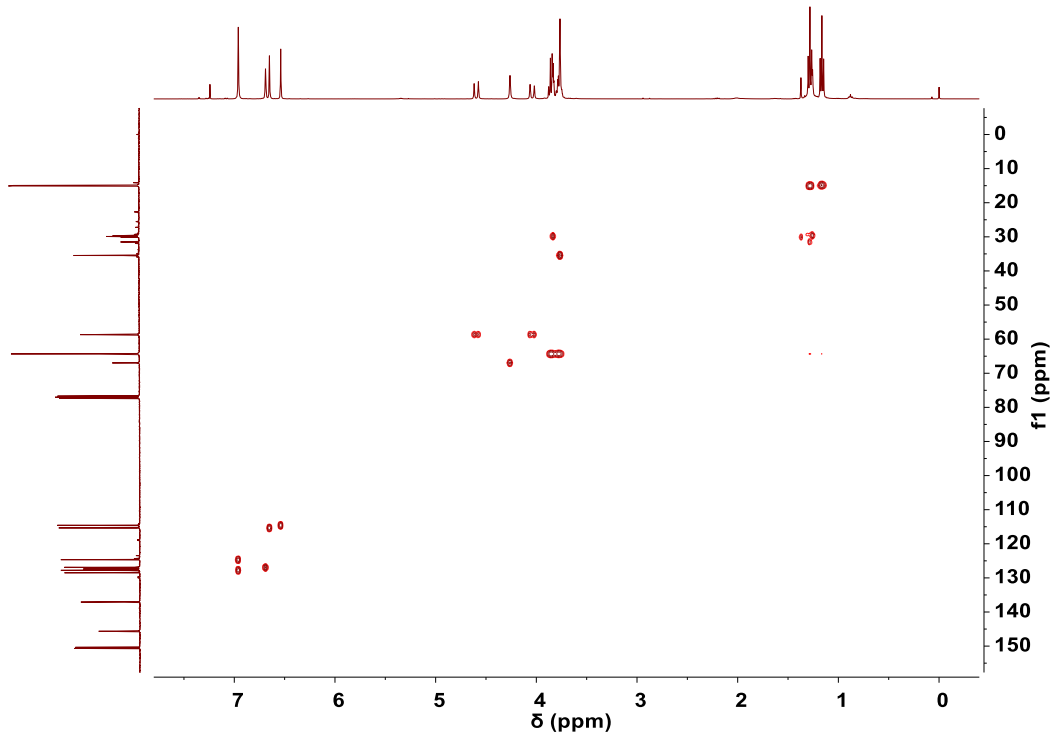

Fig. S27 HSQC NMR spectrum (100 MHz, $CDCl_3$, 298 K) of S_{6N}-**E[3]**.

3. High Resolution ESI-MS of M[3], E[3] and B[3]

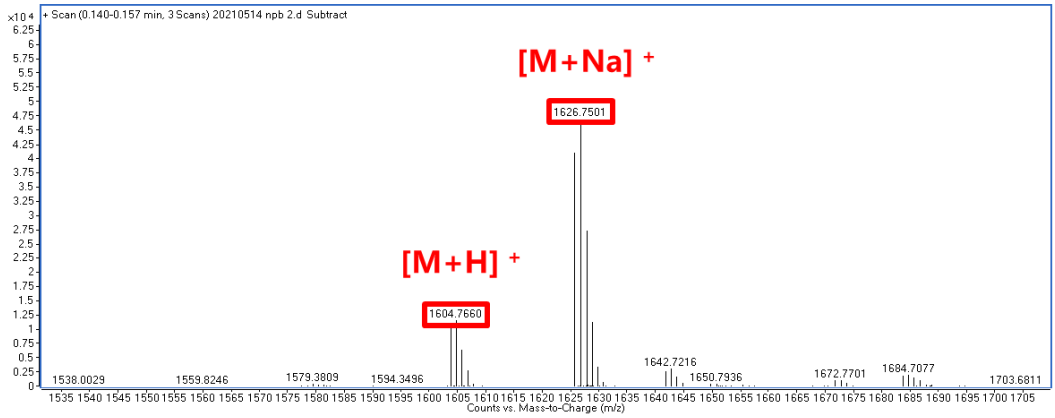

Fig. S28 High Resolution ESI-MS of **M[3]** with the parent ion $[M + H]^+$ and $[M + Na]^+$at 1604.7660 and 1626.7501, corresponding to $C_{102}H_{103}N_6O_{12}^+$ and $C_{102}H_{102}N_6NaO_{12}^+$ with the calculated *m/z* = 1604.7662 and 1626.7481.

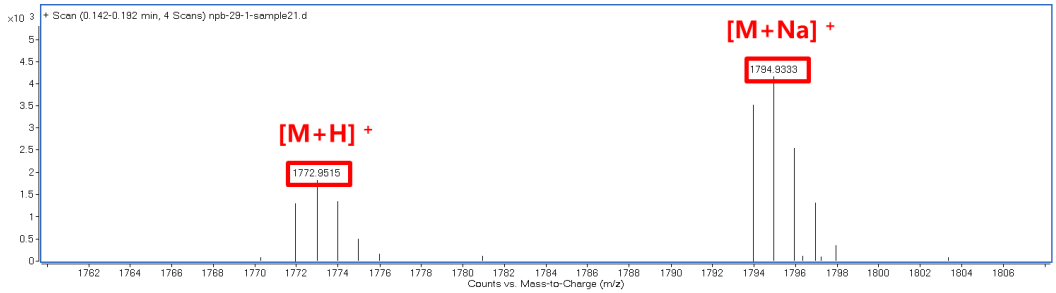

Fig. S29 High Resolution ESI-MS of **E[3]** with the parention $[M + H]^+$ and $[M + Na]^+$at 1772.9515 and 1794.9333, corresponding to $C_{114}H_{127}N_6O_{12}^+$ and $C_{114}H_{126}N_6NaO_{12}^+$ with the calculated *m/z* = 1772.9540 and 1794.9359.

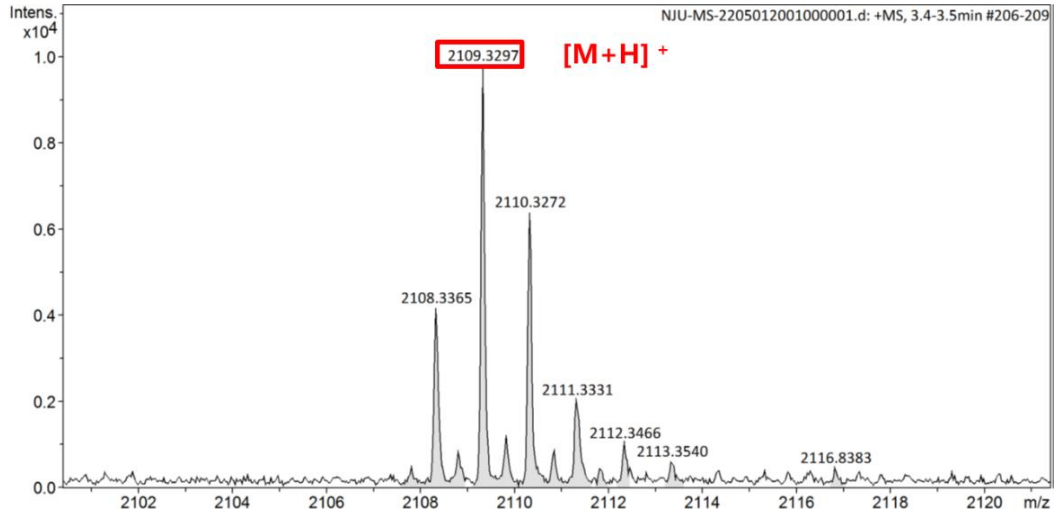

Fig. S30 High Resolution ESI-MS of **B[3]** with the parent ion $[M + H]^+$at 2109.3297, corresponding to $C_{138}H_{175}N_6O_{12}^+$ with the calculated *m/z* = 2109.3296.

4. X-ray Experimental Data for *rac*-MTB

Single crystals of *rac*-**MTB** were obtained by slow evaporation of the solution of *rac*-**MTB** in a mixed solvent of hexane and ethyl acetate at 25 °C.

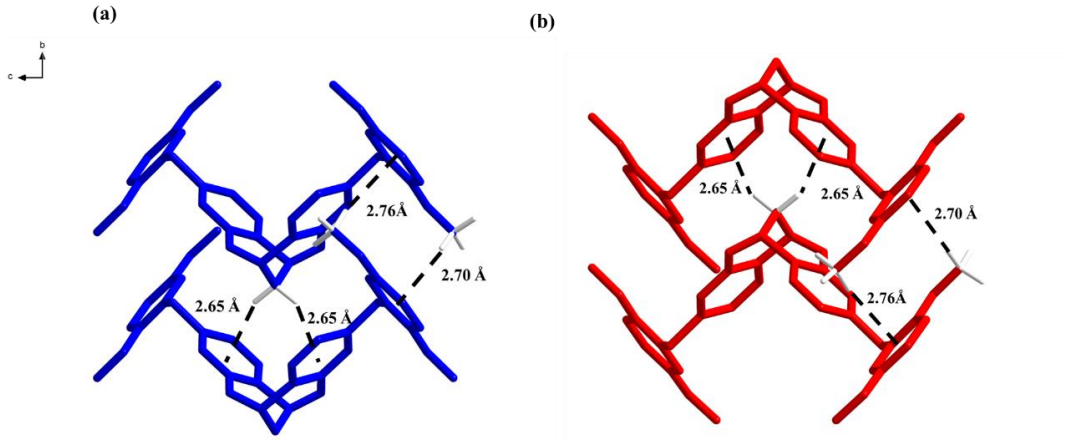

Fig. S31 The crystal structure of (a) R_{2N}-**MTB** (b) S_{2N}-**MTB**. Each type of enantiomers appears in pairs. The black dashes represent C-H···π interaction respectively.

Table S1. Experimental single crystal X-ray data for *rac*-**MTB** (CCDC number: 2224433).

Identification code	*rac*- **MTB**
Empirical formula	$C_{33}H_{34}N_2O_4$
Formula weight	522.25
Temperature/K	193.0
Crystal system	monoclinic
Space group	C2/c
a/Å	20.8793(8)
b/Å	5.2883(2)
c/Å	25.9027(10)
α/°	90
β/°	108.6850(10)
γ/°	90
Volume/Å^3	2709.33
Z	4
ρ_{calc}g/cm^3	1.281
μ/mm^{-1}	0.432
F(000)	1112.0
Crystal size/mm^3	0.22 × 0.2 × 0.19
2θ range for data collection/°	6.268 to 107.964
Index ranges	$-24 \le h \le 24$, $-6 \le k \le 6$, $-31 \le l \le 30$
Reflections collected	14157
Independent reflections	2470 [Rint = 0.0317, Rsigma = 0.0208]
Data/restraints/parameters	2470/0/231

Goodness-of-fit on F^2	1.051
Final R indexes [I>=2σ (I)]	R1 = 0.0600, wR2 = 0.1441
Final R indexes [all data]	R1 = 0.0685, wR2 = 0.1504
Largest diff. peak/hole / e Å-3	0.25/-0.46

5.Resolution of R_{2N}-ETB and S_{2N}-ETB

Sample name	Appearance	ee	Mass/g	Chromatogram at
Raw Material	white powder	--	0.6812	page 2
Peak 1	white powder	> 98%	0.2177	page 3
Peak 2	white powder	> 98%	0.2543	page 4

CHIRAL CHROMATOGRAPHY REPORT

Column	:	CHIRALPAK IG(IG00CE-UC054)
Column size	:	0.46 cm I.D. × 25 cm L
Injection	:	2 ul
Mobile phase	:	MeOH/DCM/DEA=90/10/0.1(V/V/V)
Flow rate	:	1.0 ml/min
Wave length	:	UV 214 nm
Temperature	:	35 °C
HPLC equipment	:	Shimadzu LC-20AT CP-HPLC-07
Sample name	:	Raw Material

<Chromatogram>

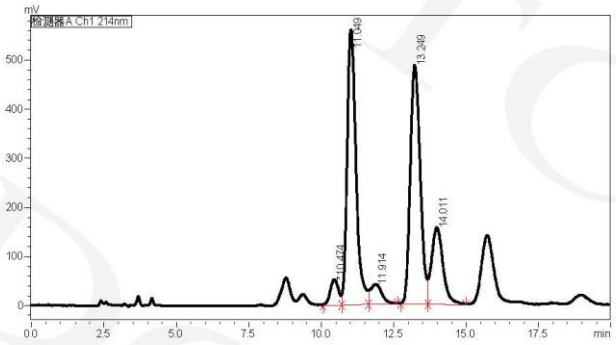

<Peak Table>

Peak#	Ret. Time	Area	Area%	T.Plate#	Tailing F.	Resolution
1	10.474	986627	3.323	5790	--	--
2	11.049	11853667	39.923	6792	1.444	1.059
3	11.914	1078918	3.634	2738	--	1.196
4	13.249	11531200	38.837	7160	--	1.736
5	14.011	4241108	14.284	5836	--	1.122

Fig. S32 chiral chromatography report of *rac*-**ETB**.

CHIRAL CHROMATOGRAPHY REPORT

Column	:	CHIRALPAK IG(IG00CE-UC054)
Column size	:	0.46 cm I.D. × 25 cm L
Injection	:	5 ul
Mobile phase	:	MeOH/DCM/DEA=90/10/0.1(V/V/V)
Flow rate	:	1.0 ml/min
Wave length	:	UV 214 nm
Temperature	:	35 °C
HPLC equipment	:	Shimadzu LC-20AT CP-HPLC-07
Sample name	:	Peak 1

<Chromatogram>

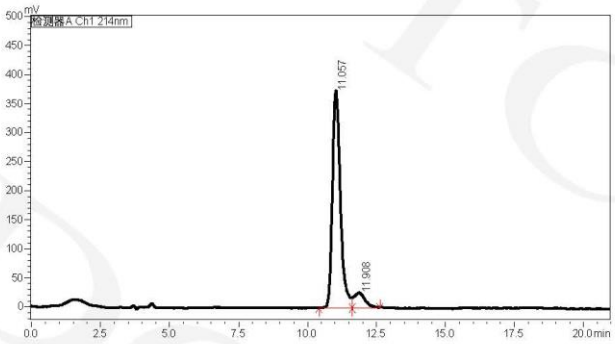

<Peak Table>

Peak#	Ret. Time	Area	Area%	T.Plate#	Tailing F.	Resolution
1	11.057	7479316	91.616	7486	1.395	--
2	11.908	684487	8.384	2198	--	1.115

Fig. S33 chiral chromatography report of S_{2N}-**ETB**.

CHIRAL CHROMATOGRAPHY REPORT

Column	:	CHIRALPAK IG(IG00CE-UC054)
Column size	:	0.46 cm I.D. × 25 cm L
Injection	:	10 ul
Mobile phase	:	MeOH/DCM/DEA=90/10/0.1(V/V/V)
Flow rate	:	1.0 ml/min
Wave length	:	UV 214 nm
Temperature	:	35 °C
HPLC equipment	:	Shimadzu LC-20AT CP-HPLC-07
Sample name	:	Peak 2

<Chromatogram>

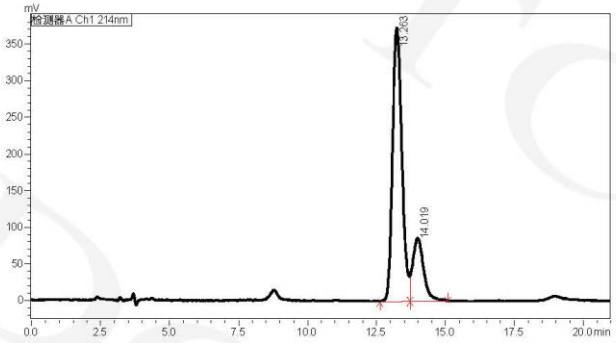

<Peak Table>

Peak#	Ret. Time	Area	Area%	T.Plate#	Tailing F.	Resolution
1	13.263	8752832	78.608	7436	--	--
2	14.019	2381943	21.392	5526	--	1.104

Fig. S34 chiral chromatography report of R_{2N}-**ETB**.

6. CD Spectra

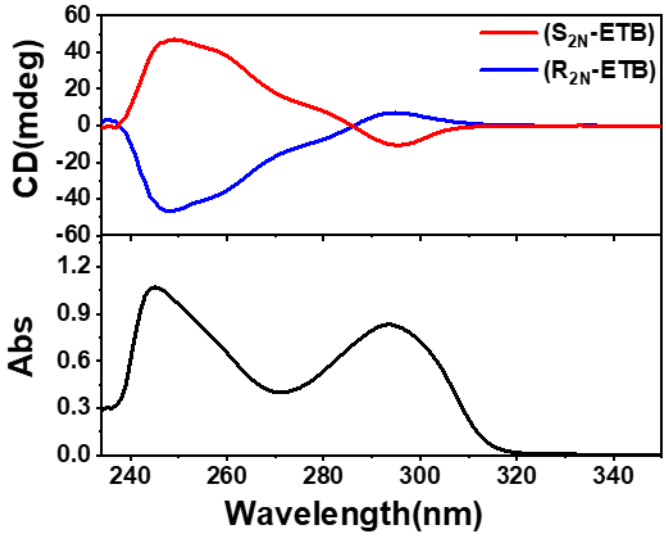

Fig. S35 CD spectra of S_{2N}-**ETB** (0.05 mM, red) and R_{2N}-**ETB** (0.05 mM, blue) in $CHCl_3$.

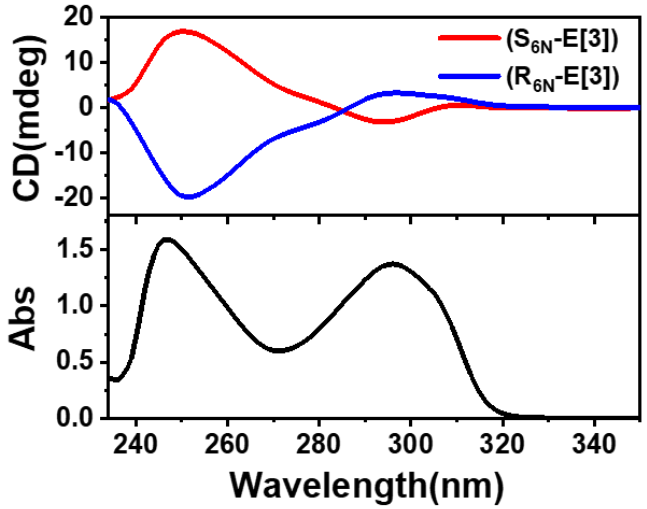

Fig. S36 CD spectra of S_{6N}-**E[3]** (0.01 mM, red) and R_{6N}-**E[3]** (0.01 mM, blue) in $CHCl_3$.

7. Iodine Vapor Adsorption Experiments

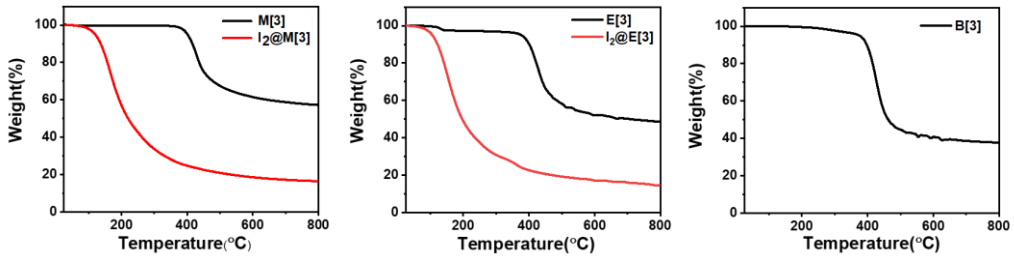

Fig. S37 Thermogravimetric analysis of (a) **M[3]**, (b) **E[3]** before and after adsorption of iodine vapor and (c) **B[3]**.

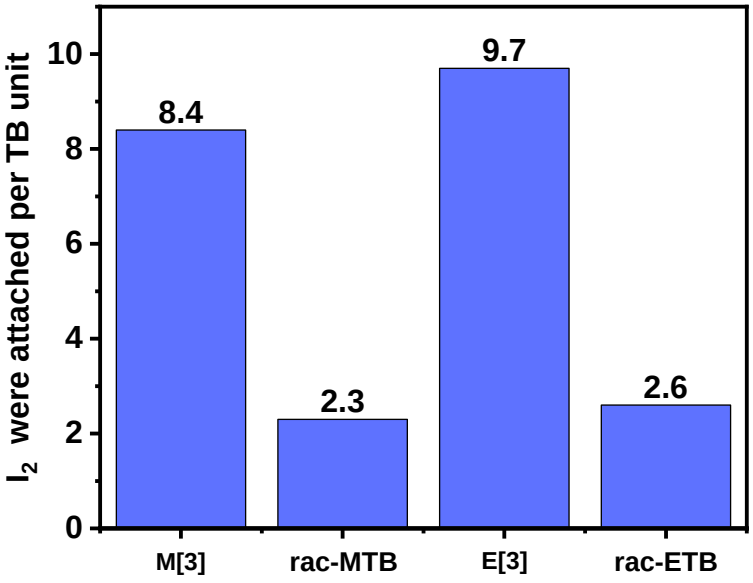

Fig. S38 iodine molecules were attached per indole unit for **M[3]**, *rac*-**MTB**, **E[3]** and *rac*-**ETB**.

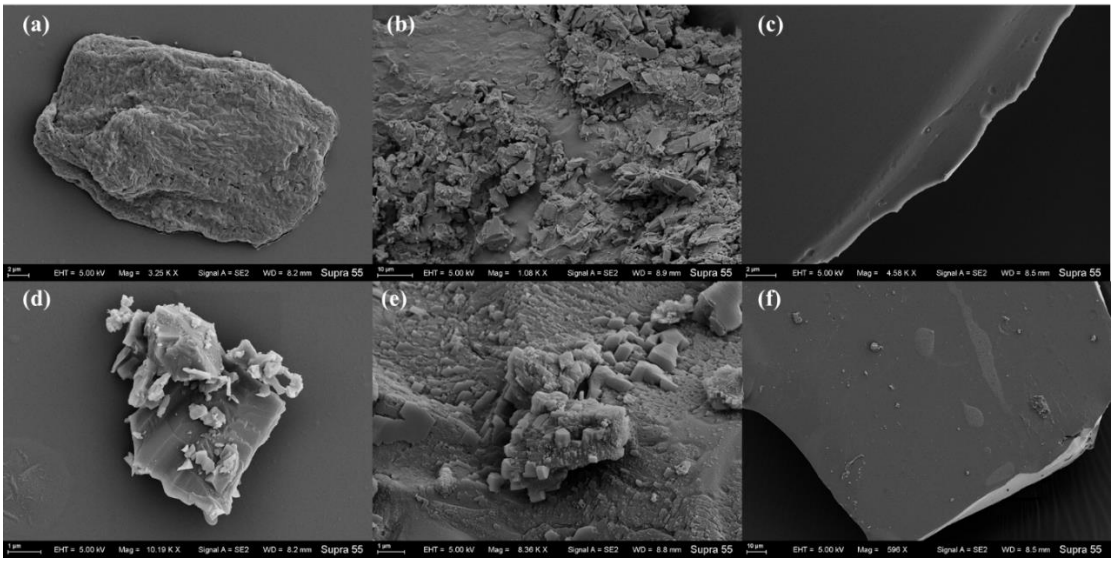

Fig. S39 Scanning electron microscopy image of **M[3]** and **E[3]**. (a) (d) before, (b) (e) after adsorption iodine, (c) (f) after desorption of iodine vapor.

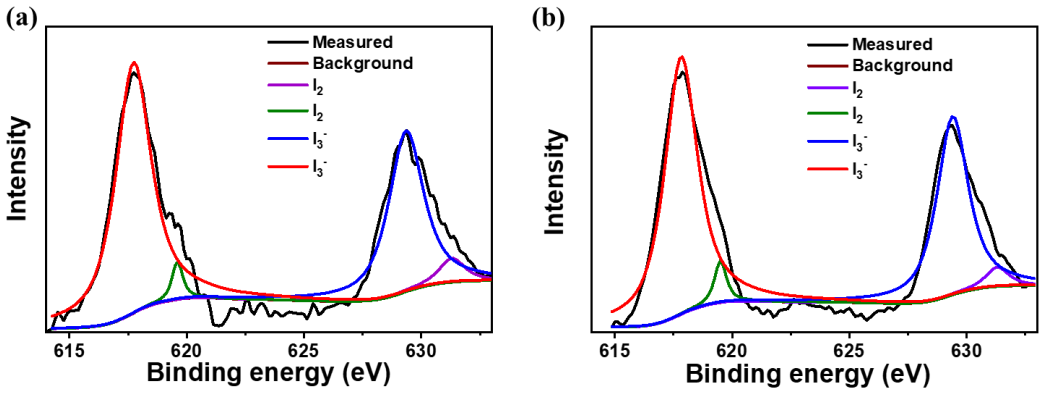

Fig. S40 High-resolution I 3d XPS spectra of (a) I_2@**M[3],** (b) I_2@**E[3]**.

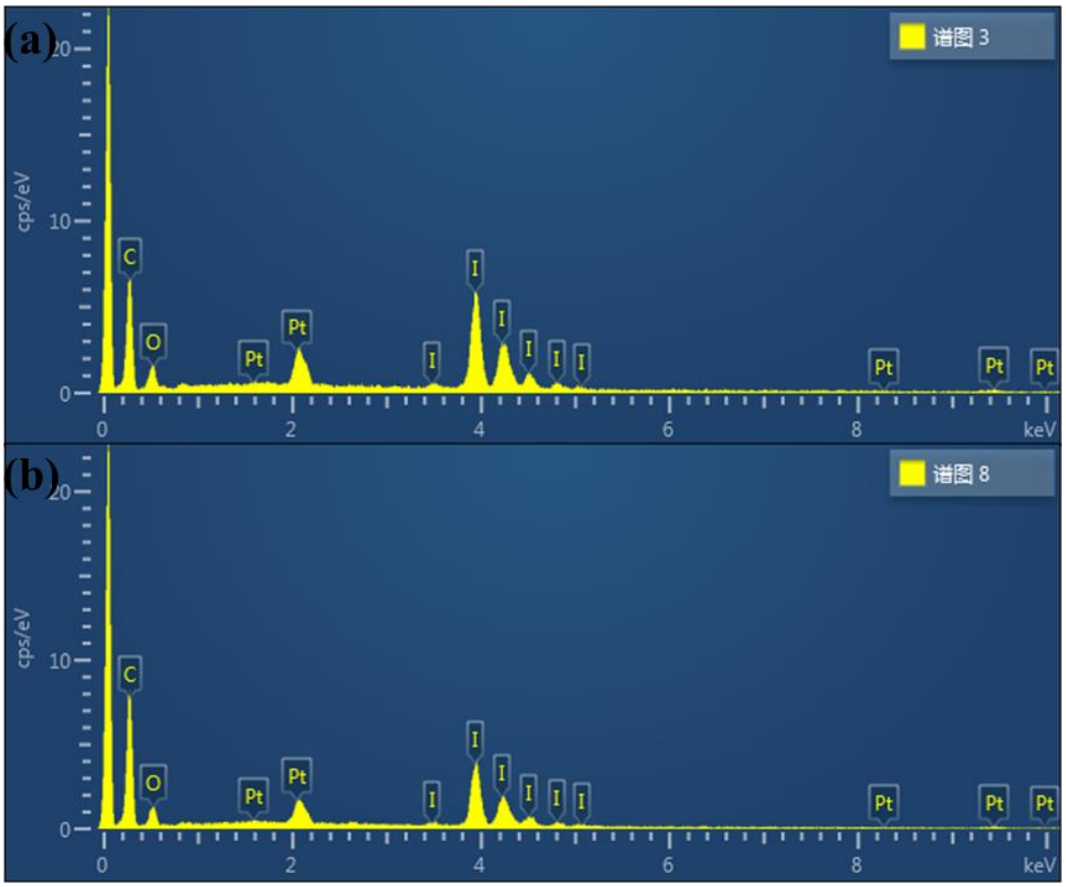

Fig. S41 Energy-dispersive spectroscopy (EDS) analysis profile of (a) **M[3],** (b) **E[3]** after adsorption of iodine vapor.

8. Iodine desorption in methanol

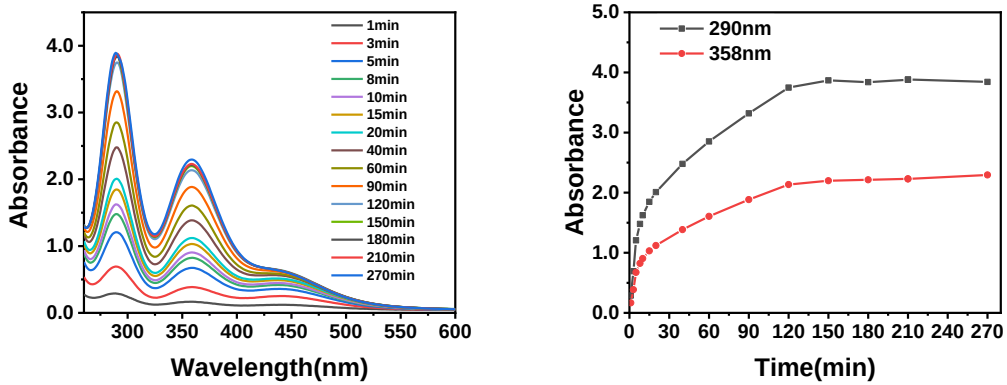

Fig. S42 Time-dependent UV/vis spectral changes after adding 2 mg I_2@**M[3]** in 10.0 mL methanol.

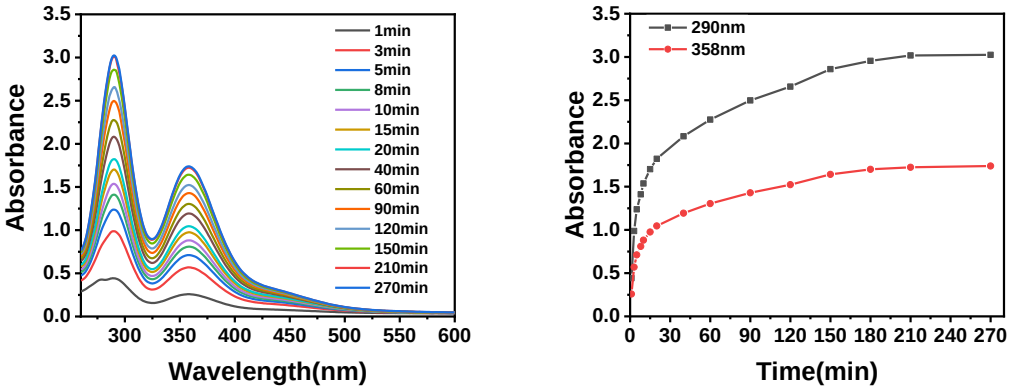

Fig. S43 Time-dependent UV/vis spectral changes after adding 2 mg I_2@**E[3]** in 10.0 mL methanol.

9. Reference

S1 D. Didier, B. Tylleman, N. Lambert, C. M. L. Vande Velde, F. Blockhuys, A. Collas and S. Sergeyev, *Tetrahedron*, 2008, **64**, 6252-6262.